

Secondary nuclei in the Galaxy

A silhouette of a person is shown on the left side of the image, looking through a telescope mounted on a tripod. The background is a vast, starry night sky with the Milky Way galaxy visible as a bright, pinkish-white band of light stretching across the upper half of the frame. The stars are scattered throughout, with some appearing as bright white dots and others as smaller, fainter points of light.

Fiorenza Donato
Torino University and INFN

Rencontres du Vietnam - Very High Energy Phenomena in the Universe
Qui Nhon, August 14, 2018

Primary and secondary cosmic rays in the Galaxy

Primaries: produced in the sources (SNR and Pulsars)

H, He, CNO, Fe; e^- , e^+

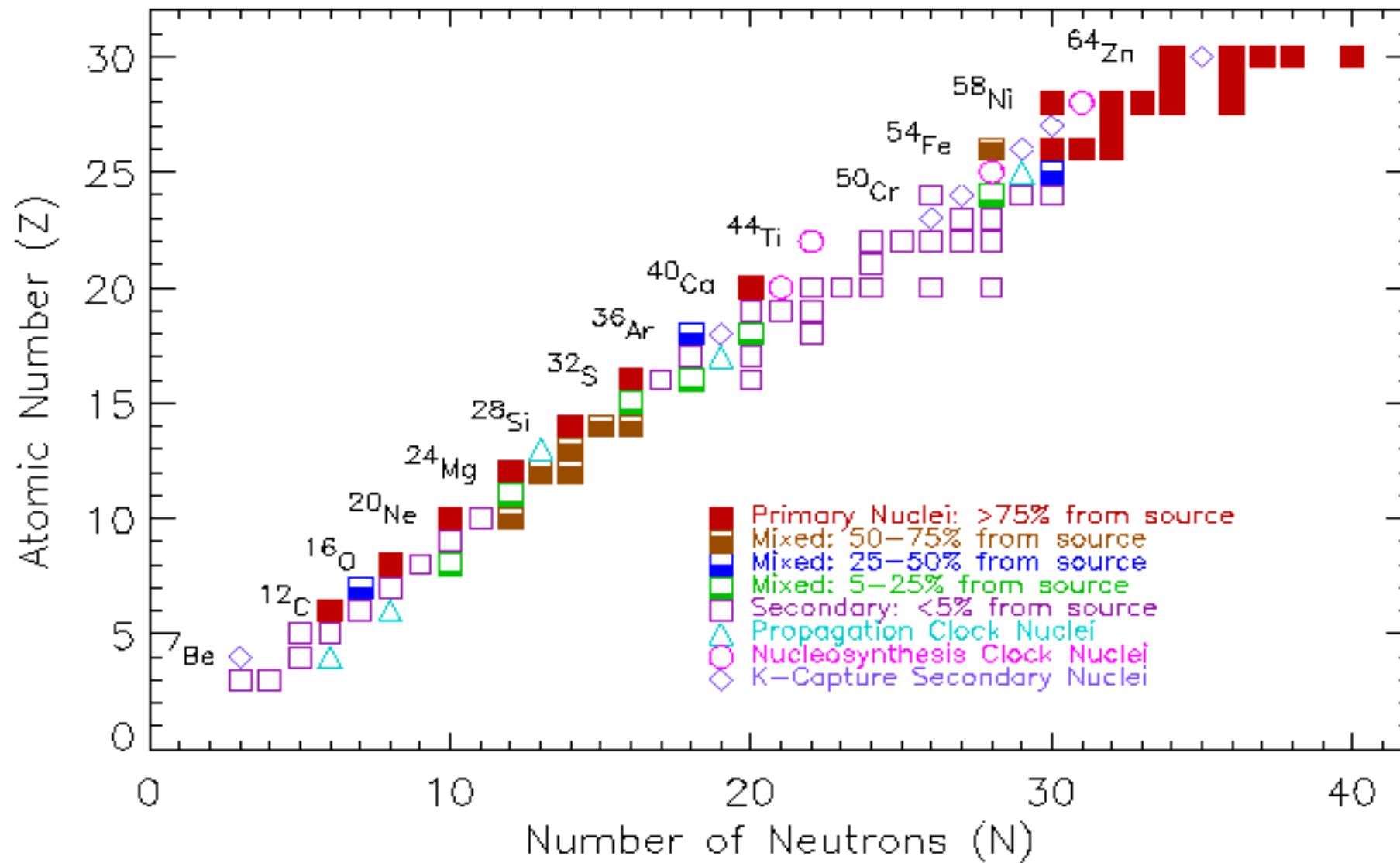
Possibly e^+ , p^- , d^- from Dark Matter annihilation

Secondaries : produced by spallation of primary CRs (p, He, C, O, Fe) on the interstellar medium (ISM)

LiBeB, sub-Fe; e^+ , p^- , d^-

All primary and secondary species propagate in the Galaxy, dominated by diffusion on the magnetic fields and/or by intense energy losses (leptons)

Primary - mixed - secondary nuclei



Li - Be - B are fully secondary, ^{12}C and ^{16}O primary. Many are mixed.
Isotopes are relevant (^{10}Be)

Transport equation in diffusion models for flux (intensity) $N^j(E)$

$$\Gamma^j = \Gamma^{j,\text{inel}} + \Gamma^{j,\text{rad}}$$

$$-\vec{\nabla} \left[K \vec{\nabla} N^j(E) - \vec{V}_c N^j(E) \right] - \Gamma^j N^j$$

Primary production
(SNR, PSR, DM)

$$-\frac{(\vec{\nabla} \cdot \vec{V}_c)}{3} \frac{\partial}{\partial E} \left[\frac{p^2}{E} N^j(E) \right] = Q^j(E) +$$

$$\bar{Q}^j \equiv q_0^j Q(E) \hat{q}_i + \sum_k^{m_k > m_j} \tilde{\Gamma}^{kj} N_i^k(0)$$

Secondary production
by fragmentation

$$\frac{\partial}{\partial E} \left[-b_{\text{tot}}(E) N^j(E) + \beta^2 K_{pp} \frac{\partial N^j(E)}{\partial E} \right]$$

$$b_{\text{tot}} = b_{\text{loss}} + b_{\text{reac}}$$

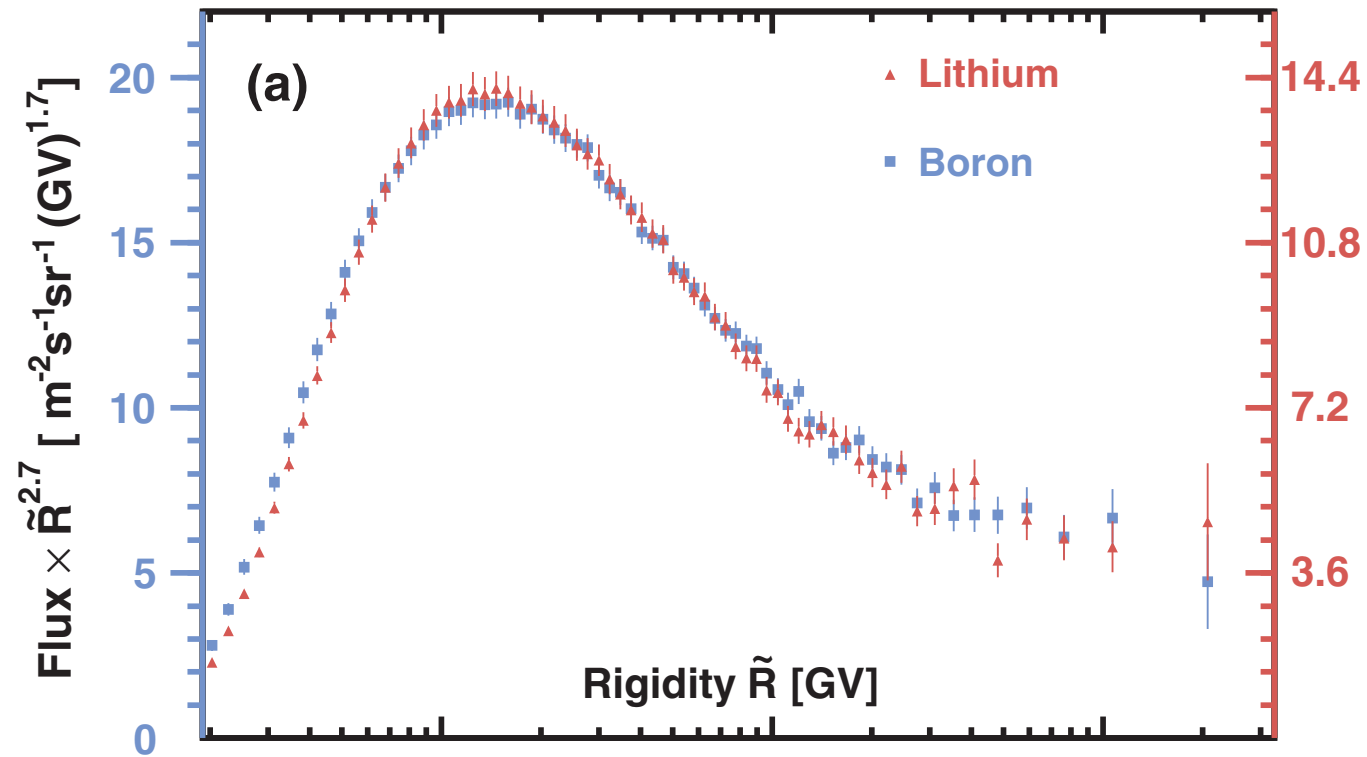
$$b_{\text{loss}}(E) = \left(\frac{dE}{dt} \right)_{\text{Ion}} + \left(\frac{dE}{dt} \right)_{\text{Coul}} + \left(\frac{dE}{dt} \right)_{\text{Adiab}}$$

It is a second order differential equation in space and in energy

Secondary fluxes are grossly proportional to their
production cross sections and parent nucleus flux

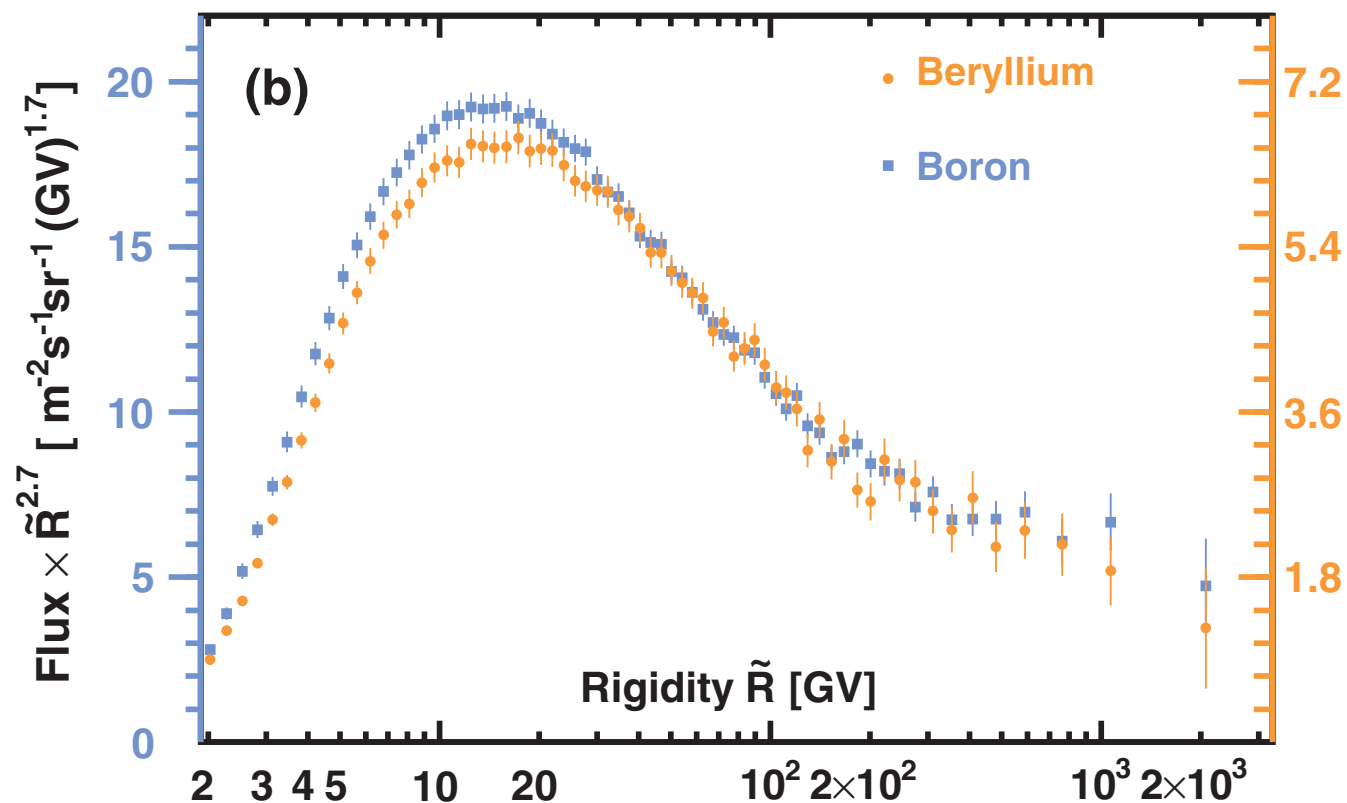
The Lithium - Berillium - Boron secondary nuclei

AMS Collaboration, Phys. Rev Lett. 2018



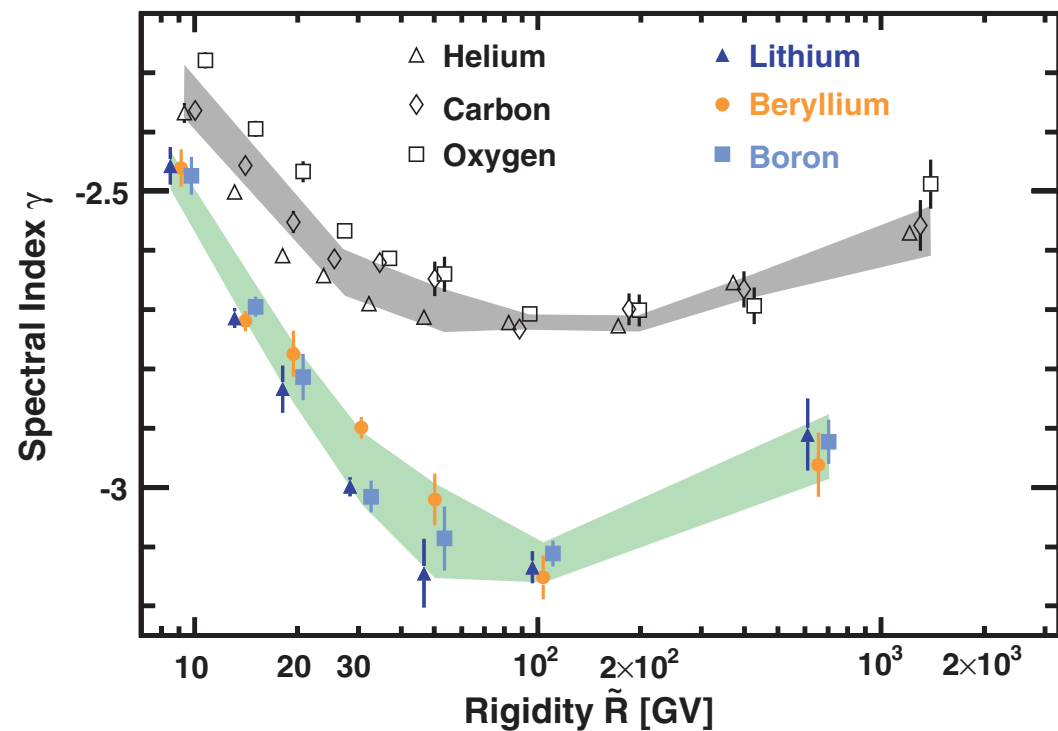
Lithium and Boron have the same rigidity dependence above 7 GV.

All the three secondary nuclei have the same rigidity dependence above 30 GV.



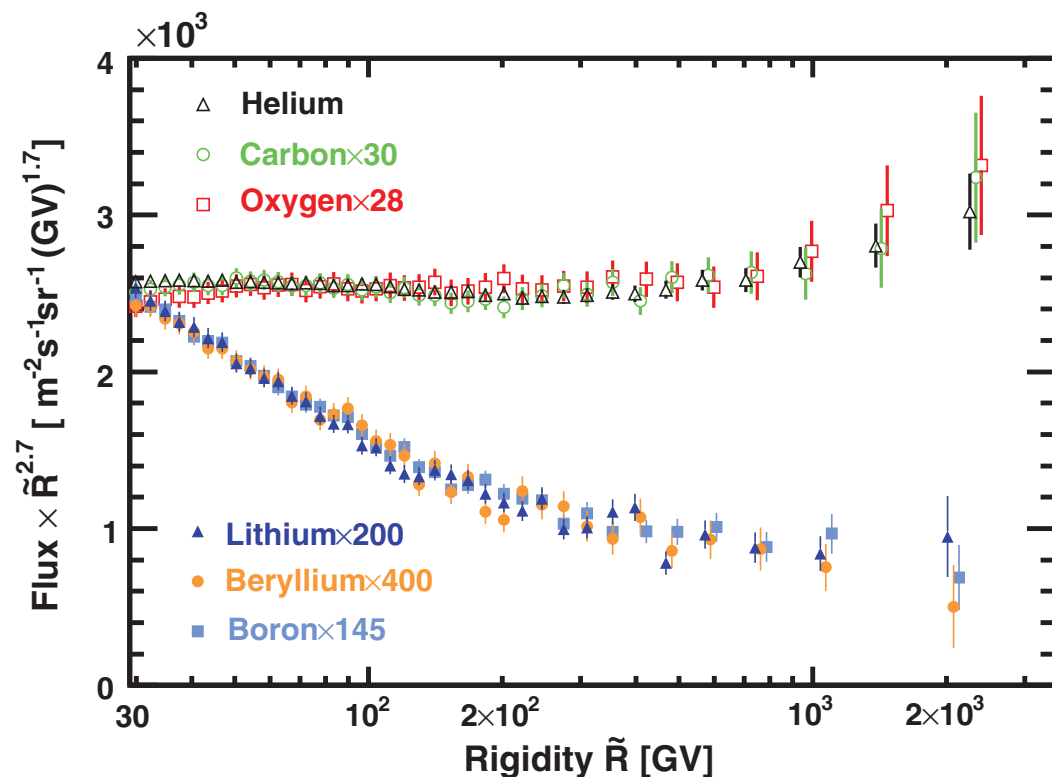
The different Be behavior is due to the presence of the radioactive ^{10}Be isotope, with a lifetime of 1.4 MY

A spectral break in the observed fluxes



The rigidity dependence of Li, Be and B are nearly identical, but different from the primary He, C and O (and also p).

Li, Be, B fluxes measured by Pamela and AMS show an identical hardening w.r.t. energy above 200 GV.



The spectral index of secondaries hardens 0.13 \pm 0.03 more than for primaries

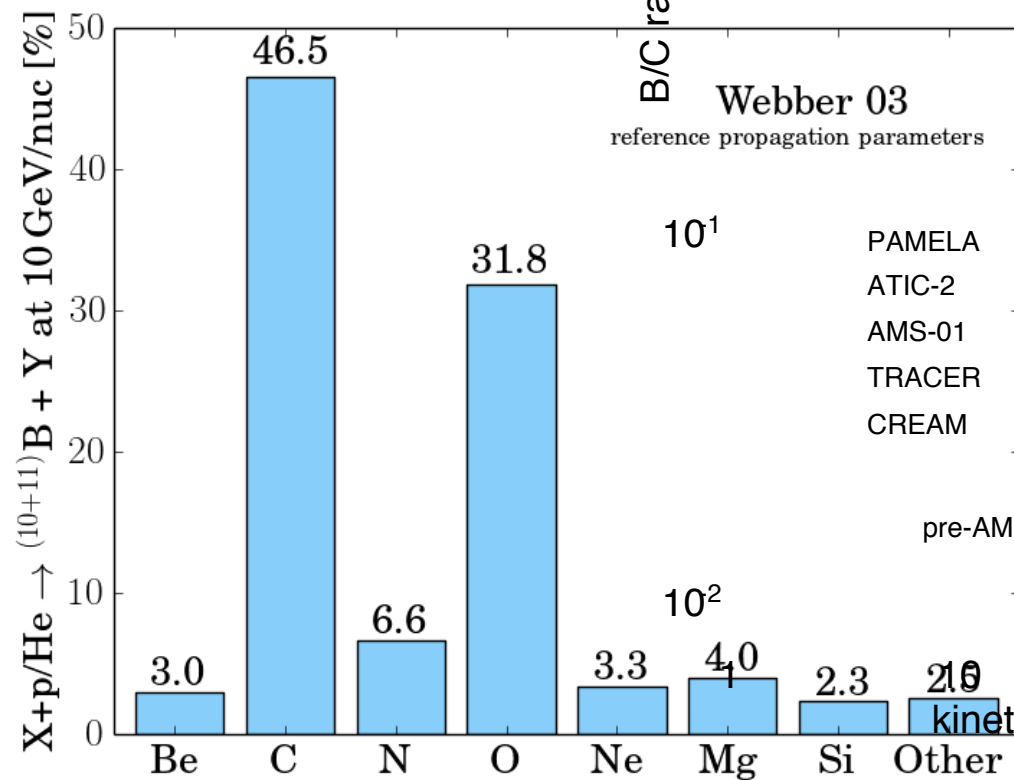
See D. Grasso talk

Boron-to-Carbon: a standard candle for fixing GALACTIC PROPAGATION

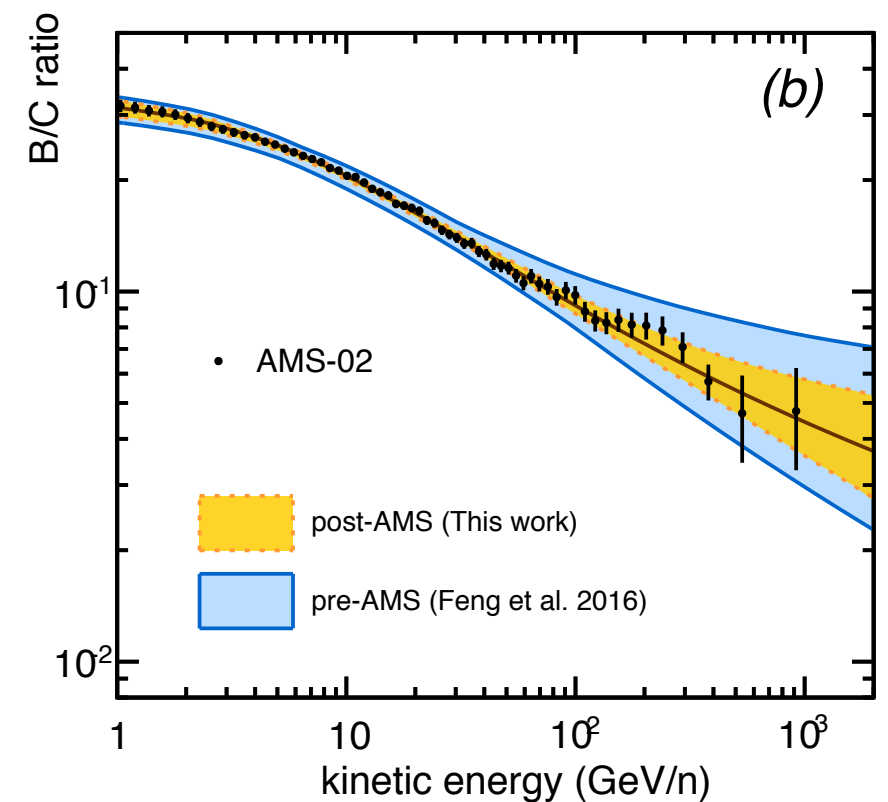
Li, Be, B are produced by fragmentation
of heavier nuclei (mostly C, N, O)
on H and He: production cross sections

B/C is very sensitive to **propagation effects**, kind of standard candle

Genolini, Putze, Serpico, Salati 2015



Tomassetti, Feng, Oliva PRD 2017



B/C (AMS, PRL 117, 2016) does not show features at high energies

Production cross sections in the galactic cosmic ray modeling

H, He, C, O, Fe,... are present in the supernova remnant surroundings, and directly accelerated into the the interstellar medium (ISM)

All the other nuclei (Li, Be, B, p-, and e+, gamma, ...) are produced by spallation of heavier nuclei with the atoms (H, He) of the ISM

We need all the cross sections σ^{kj} - from Nickel down to proton - for the production of the j-particle from the heavier k-nucleus scattering off the H and He of the ISM

Remarkable for DARK MATTER signals is productions of: antiproton, antideuteron, positron and gamma rays.

Current status and desired accuracy of the isotopic production cross sections relevant to astrophysics of cosmic rays I. Li, Be, B, C, N

Yoann Génolini*

Service de Physique Théorique, Université Libre de Bruxelles,
Boulevard du Triomphe, CP225, 1050 Brussels, Belgium

arxiv: 1803.04685

David Maurin†

LPSC, Université Grenoble-Alpes, CNRS/IN2P3, 53 avenue des Martyrs, 38026 Grenoble, France

Igor V. Moskalenko‡

W. W. Hansen Experimental Physics Laboratory and Kavli Institute for Particle
Astrophysics and Cosmology, Stanford University, Stanford, CA 94305, USA

Michael Unger§

Karlsruhe Institute of Technology, Karlsruhe, Germany
(Dated: March 14, 2018)

- Ranking of the most important cross sections for the production of Li, Be, B, C, N
- Propagation of uncertainties

Reaction $a + b \rightarrow c$	Flux impact f_{abc} [%]			σ [mb]	Data	σ/σ
	min	mean	max			
$\sigma(^{12}\text{C} + \text{H} \rightarrow ^6\text{Li})$	11.0	13.6	16.0	14.0	✓	
$\sigma(^{16}\text{O} + \text{H} \rightarrow ^6\text{Li})$	11.0	13.5	16.0	13.0	✓	
$\sigma(^{12}\text{C} + \text{H} \rightarrow ^7\text{Li})$	10.0	11.9	14.0	12.6	✓	
$\sigma(^{16}\text{O} + \text{H} \rightarrow ^7\text{Li})$	9.6	11.3	13.0	11.2	✓	
$\sigma(^{11}\text{B} + \text{H} \rightarrow ^7\text{Li})$	3.00	3.52	4.00	21.5	✓	
$\sigma(^{13}\text{C} + \text{H} \rightarrow ^7\text{Li})$	2.00	2.39	2.80	22.1		
$\sigma(^{16}\text{O} + \text{H} \rightarrow ^9\text{Li})$	2.00	2.38	2.80	20.6		
$\sigma(^7\text{Li} + \text{H} \rightarrow ^6\text{Li})$	2.30	2.35	2.40	31.5	✓	
$\sigma(^{12}\text{C} + \text{He} \rightarrow ^6\text{Li})$	1.90	2.33	2.70	21.6		
$\sigma(^{12}\text{C} + \text{H} \rightarrow ^7\text{Li})$	1.90	2.27	2.60	18.6	✓	
$\sigma(^{12}\text{C} + \text{He} \rightarrow ^7\text{Li})$	1.70	2.04	2.40	19.4		
$\sigma(^{16}\text{O} + \text{He} \rightarrow ^7\text{Li})$	1.70	2.00	2.30	17.8		
$\sigma(^{24}\text{Mg} + \text{H} \rightarrow ^7\text{Li})$	1.70	1.98	2.30	12.6		
$\sigma(^{13}\text{C} + \text{H} \rightarrow ^6\text{Li})$	1.60	1.97	2.30	17.8		
$\sigma(^{24}\text{Mg} + \text{H} \rightarrow ^6\text{Li})$	1.50	1.74	2.00	11.4		
$\sigma(^{10}\text{B} + \text{H} \rightarrow ^6\text{Li})$	1.40	1.64	1.90	20.0		
$\sigma(^{14}\text{N} + \text{H} \rightarrow ^6\text{Li})$	1.40	1.62	1.90	13.0	✓	
$\sigma(^{15}\text{N} + \text{H} \rightarrow ^6\text{Li})$	1.30	1.60	1.90	12.8	✓	
$\sigma(^{12}\text{C} + \text{H} \rightarrow ^{11}\text{B})$	1.20	1.38	1.60	30.0	✓	1.8
$\sigma(^7\text{Be} + \text{H} \rightarrow ^6\text{Li})$	1.20	1.34	1.50	21.0		
$\sigma(^{12}\text{C} + \text{H} \rightarrow ^{11}\text{C})$	1.10	1.24	1.40	26.9	✓	n/a
$\sigma(^{14}\text{N} + \text{H} \rightarrow ^7\text{Li})$	0.95	1.13	1.30	9.3	✓	
$\sigma(^{56}\text{Fe} + \text{H} \rightarrow ^7\text{Li})$	0.00	0.94	1.90	[0.0, 23.0]		
$\sigma(^{56}\text{Fe} + \text{H} \rightarrow ^6\text{Li})$	0.00	0.94	1.90	[0.0, 22.0]		
$\sigma(^{16}\text{O} + \text{H} \rightarrow ^{11}\text{B})$	0.80	0.90	1.00	18.2	✓	1.5
$\sigma(^{11}\text{B} + \text{H} \rightarrow ^6\text{Li})$	0.71	0.84	0.97	5.0	✓	
$\sigma(^{28}\text{Si} + \text{H} \rightarrow ^6\text{Li})$	0.00	0.80	1.60	[0.0, 13.0]		
$\sigma(^{10}\text{B} + \text{H} \rightarrow ^7\text{Li})$	0.70	0.80	0.90	10.0		
$\sigma(^{28}\text{Si} + \text{H} \rightarrow ^7\text{Li})$	0.00	0.71	1.40	[0.0, 11.0]		
$\sigma(^{16}\text{O} + \text{H} \rightarrow ^{15}\text{N})$	0.57	0.64	0.71	34.3	✓	1.8
$\sigma(^{12}\text{C} + \text{H} \rightarrow ^{10}\text{B})$	0.53	0.64	0.74	12.3	✓	1.1
$\sigma(^{20}\text{Ne} + \text{H} \rightarrow ^6\text{Li})$	0.00	0.63	1.30	[0.0, 13.0]		
$\sigma(^{16}\text{O} + \text{H} \rightarrow ^{13}\text{O})$	0.00	0.63	0.71	30.5	✓	n/a
$\sigma(^{16}\text{O} + \text{H} \rightarrow ^{10}\text{B})$	0.50	0.60	0.70	10.9	✓	
$\sigma(^{11}\text{B} + \text{He} \rightarrow ^7\text{Li})$	0.52	0.60	0.69	33.2		
$\sigma(^{16}\text{O} + \text{H} \rightarrow ^{15}\text{O})$	0.51	0.57	0.63	30.5	✓	n/a
$\sigma(^{20}\text{Ne} + \text{H} \rightarrow ^7\text{Li})$	0.00	0.56	1.10	[0.0, 11.0]		
$\sigma(^{16}\text{O} + \text{H} \rightarrow ^7\text{Be})$	0.37	0.45	0.54	10.0	✓	
$\sigma(^{16}\text{O} + \text{H} \rightarrow ^{11}\text{C})$	0.40	0.45	0.50	9.1		n/a
$\sigma(^{56}\text{Fe} + \text{He} \rightarrow ^7\text{Li})$	0.00	0.44	0.88	[0.0, 97.0]		
$\sigma(^{56}\text{Fe} + \text{He} \rightarrow ^6\text{Li})$	0.00	0.44	0.88	[0.0, 95.0]		
$\sigma(^7\text{Li} + \text{He} \rightarrow ^6\text{Li})$	0.42	0.43	0.45	52.2		
$\sigma(^{13}\text{C} + \text{He} \rightarrow ^7\text{Li})$	0.34	0.41	0.48	34.2		
$\sigma(^{12}\text{C} + \text{H} \rightarrow ^7\text{Be})$	0.34	0.41	0.48	9.7	✓	
$\sigma(^{16}\text{O} + \text{H} \rightarrow ^{13}\text{C})$	0.36	0.41	0.46	17.5	✓	1.2
$\sigma(^{24}\text{Mg} + \text{He} \rightarrow ^6\text{Li})$	0.33	0.39	0.46	22.5		
$\sigma(^{15}\text{N} + \text{He} \rightarrow ^7\text{Li})$	0.33	0.39	0.45	28.6		
$\sigma(^7\text{Li} + \text{H} \rightarrow ^6\text{He})$	0.00	0.38	0.76	[0.0, 10.0]		n/a
$\sigma(^{11}\text{B} + \text{H} \rightarrow ^{10}\text{B})$	0.29	0.35	0.40	38.9	✓	
$\sigma(^{24}\text{Mg} + \text{He} \rightarrow ^7\text{Li})$	0.29	0.34	0.40	20.3		
$\sigma(^{13}\text{C} + \text{He} \rightarrow ^6\text{Li})$	0.28	0.34	0.40	27.5		
$\sigma(^{56}\text{Fe} + \text{H} \rightarrow ^6\text{He})$	0.00	0.29	0.57	[0.0, 6.9]		n/a

Reaction $a + b \rightarrow c$	Flux impact f_{abc} [%]			σ [mb]	Data	σ/σ
	min	mean	max			
$\sigma(^{16}\text{O} + \text{H} \rightarrow ^7\text{Be})$	17.0	17.6	19.0	10.0	✓	
$\sigma(^{12}\text{C} + \text{H} \rightarrow ^7\text{Be})$	15.0	15.9	17.0	9.7	✓	
$\sigma(^{16}\text{O} + \text{H} \rightarrow ^9\text{Be})$	8.80	9.27	9.80	6.8	✓	
$\sigma(^{16}\text{O} + \text{H} \rightarrow ^9\text{Be})$	5.00	5.34	5.60	3.7	✓	
$\sigma(^{28}\text{Si} + \text{H} \rightarrow ^7\text{Be})$	2.70	2.87	3.00	14.7		
$\sigma(^{28}\text{Si} + \text{H} \rightarrow ^7\text{Be})$	2.60	2.77	2.90	10.8		
$\sigma(^{24}\text{Mg} + \text{H} \rightarrow ^7\text{Be})$	2.50	2.65	2.80	10.0		
$\sigma(^{12}\text{C} + \text{He} \rightarrow ^7\text{Be})$	2.30	2.48	2.60	13.7		
$\sigma(^{11}\text{B} + \text{H} \rightarrow ^9\text{Be})$	2.30	2.36	2.50	10.0	✓	
$\sigma(^{12}\text{C} + \text{H} \rightarrow ^{10}\text{Be})$	2.00	2.16	2.30	4.0		
$\sigma(^{14}\text{N} + \text{H} \rightarrow ^9\text{Be})$	2.00	2.12	2.20	10.1	✓	
$\sigma(^{20}\text{Ne} + \text{H} \rightarrow ^9\text{Be})$	1.60	1.73	1.90	[7.4, 9.7]		
$\sigma(^{10}\text{B} + \text{H} \rightarrow ^9\text{Be})$	1.60	1.62	1.70	13.9		
$\sigma(^{12}\text{C} + \text{He} \rightarrow ^9\text{Be})$	1.40	1.45	1.50	9.6		
$\sigma(^{12}\text{C} + \text{H} \rightarrow ^{11}\text{B})$	1.30	1.43	1.60	30.0	✓	1.8
$\sigma(^{15}\text{N} + \text{H} \rightarrow ^9\text{Be})$	1.20	1.29	1.40	7.3		
$\sigma(^{12}\text{C} + \text{H} \rightarrow ^{11}\text{C})$	1.20	1.28	1.40	26.9	✓	n/a
$\sigma(^{16}\text{O} + \text{H} \rightarrow ^{10}\text{Be})$	1.20	1.27	1.40	2.2	✓	
$\sigma(^{11}\text{B} + \text{H} \rightarrow ^{10}\text{Be})$	1.10	1.21	1.30	12.9	✓	
$\sigma(^{11}\text{B} + \text{H} \rightarrow ^7\text{Be})$	0.99	1.16	1.30	[3.6, 4.5]	✓	
$\sigma(^{15}\text{N} + \text{H} \rightarrow ^9\text{Be})$	1.10	1.15	1.20	5.4	✓	
$\sigma(^{13}\text{C} + \text{H} \rightarrow ^9\text{Be})$	0.96	1.03	1.10	6.7	✓	
$\sigma(^{28}\text{Si} + \text{H} \rightarrow ^9\text{Be})$	0.91	0.96	1.00	4.5	✓	
$\sigma(^{10}\text{B} + \text{H} \rightarrow ^9\text{Be})$	0.93	0.95	0.98	6.9	✓	
$\sigma(^{24}\text{Mg} + \text{H} \rightarrow ^9\text{Be})$	0.89	0.94	0.99	4.3	✓	
$\sigma(^{16}\text{O} + \text{H} \rightarrow ^{11}\text{B})$	0.87	0.94	1.00	18.2	✓	1.5
$\sigma(^{56}\text{Fe} + \text{H} \rightarrow ^7\text{Be})$	0.11	0.92	1.70	[0.6, 11.0]		
$\sigma(^{16}\text{O} + \text{He} \rightarrow ^9\text{Be})$	0.82	0.87	0.92	5.4		
$\sigma(^{13}\text{C} + \text{H} \rightarrow ^7\text{Be})$	0.71	0.76	0.81	4.1	✓	
$\sigma(^{20}\text{Ne} + \text{H} \rightarrow ^9\text{Be})$	0.68	0.72	0.76	4.3		
$\sigma(^{12}\text{C} + \text{H} \rightarrow ^{10}\text{B})$	0.59	0.64	0.68	12.3	✓	1.1
$\sigma(^{16}\text{O} + \text{H} \rightarrow ^{10}\text{B})$	0.56	0.60	0.65	10.9	✓	
$\sigma(^9\text{Be} + \text{H} \rightarrow ^7\text{Be})$	0.59	0.59	0.60	10.6	✓	
$\sigma(^{28}\text{Si} + \text{He} \rightarrow ^7\text{Be})$	0.53	0.56	0.60	19.8		
$\sigma(^{56}\text{Fe} + \text{H} \rightarrow ^9\text{Be})$	0.06	0.53	1.00	[0.4, 7.5]		
$\sigma(^{24}\text{Mg} + \text{He} \rightarrow ^7\text{Be})$	0.47	0.50	0.52	16.8		
$\sigma(^{16}\text{O} + \text{H} \rightarrow ^{11}\text{C})$	0.43	0.47	0.50	9.1		n/a
$\sigma(^{16}\text{O} + \text{H} \rightarrow ^{15}\text{N})$	0.41	0.44	0.47	34.3	✓	1.8
$\sigma(^{56}\text{Fe} + \text{He} \rightarrow ^7\text{Be})$	0.05	0.41	0.77	[2.4, 43.0]		
$\sigma(^{16}\text{O} + \text{H} \rightarrow ^{15}\text{O})$	0.37	0.39	0.42	30.5	✓	n/a
$\sigma(^{27}\text{Al} + \text{H} \rightarrow ^7\text{Be})$	0.30	0.38	0.45	[5.3, 8.9]		
$\sigma(^{14}\text{N} + \text{H} \rightarrow ^9\text{Be})$	0.35	0.37	0.39	2.1	✓	
$\sigma(^{11}\text{B} + \text{He} \rightarrow ^9\text{Be})$	0.35	0.37	0.38	14.0		
$\sigma(^{13}\text{C} + \text{H} \rightarrow ^{10}\text{Be})$	0.33	0.33	0.40	5.9	✓	
$\sigma(^{11}\text{B} + \text{H} \rightarrow ^7\text{Be})$	0.30	0.35	0.41	[5.8, 8.6]		
$\sigma(^{11}\text{B} + \text{H} \rightarrow ^{10}\text{B})$	0.33	0.35	0.37	38.9	✓	
$\sigma(^{25}\text{Mg} + \text{H} \rightarrow ^{10}\text{Be})$	0.29	0.34	0.40	[5.6, 8.8]		
$\sigma(^{14}\text{C} + \text{He} \rightarrow ^7\text{Be})$	0.31	0.34	0.36	5.6		
$\sigma(^{14}\text{N} + \text{He} \rightarrow ^7\text{Be})$	0.32	0.34	0.36	14.4		
$\sigma(^{20}\text{Ne} + \text{He} \rightarrow ^7\text{Be})$	0.28	0.30	0.32	[12.0, 15.0]		
$\sigma(^{22}\text{Ne} + \text{H} \rightarrow ^7\text{Be})$	0.22	0.25	0.28	[4.7, 6.4]		
$\sigma(^{10}\text{B} + \text{He} \rightarrow ^9\text{Be})$	0.25	0.25	0.26	19.6		
$\sigma(^{26}\text{Mg} + \text{H} \rightarrow ^7\text{Be})$	0.21	0.25	0.29	[4.7, 7.2]		
$\sigma(^{16}\text{O} + \text{H} \rightarrow ^9\text{Li})$	0.23	0.24	0.26	0.3	✓	n/a

# of channels	in range	contribution [%]		
		min	mean	max
13	[1%,100%]			82.2
25	[0.1%,1%]			7.7
110	[0.01%,0.1%]			3.8
346	[0.001%,0.01%]			1.3
526	[0.0001%,0.001%]			0.2
2340	[0.0%,0.0001%]			0.0

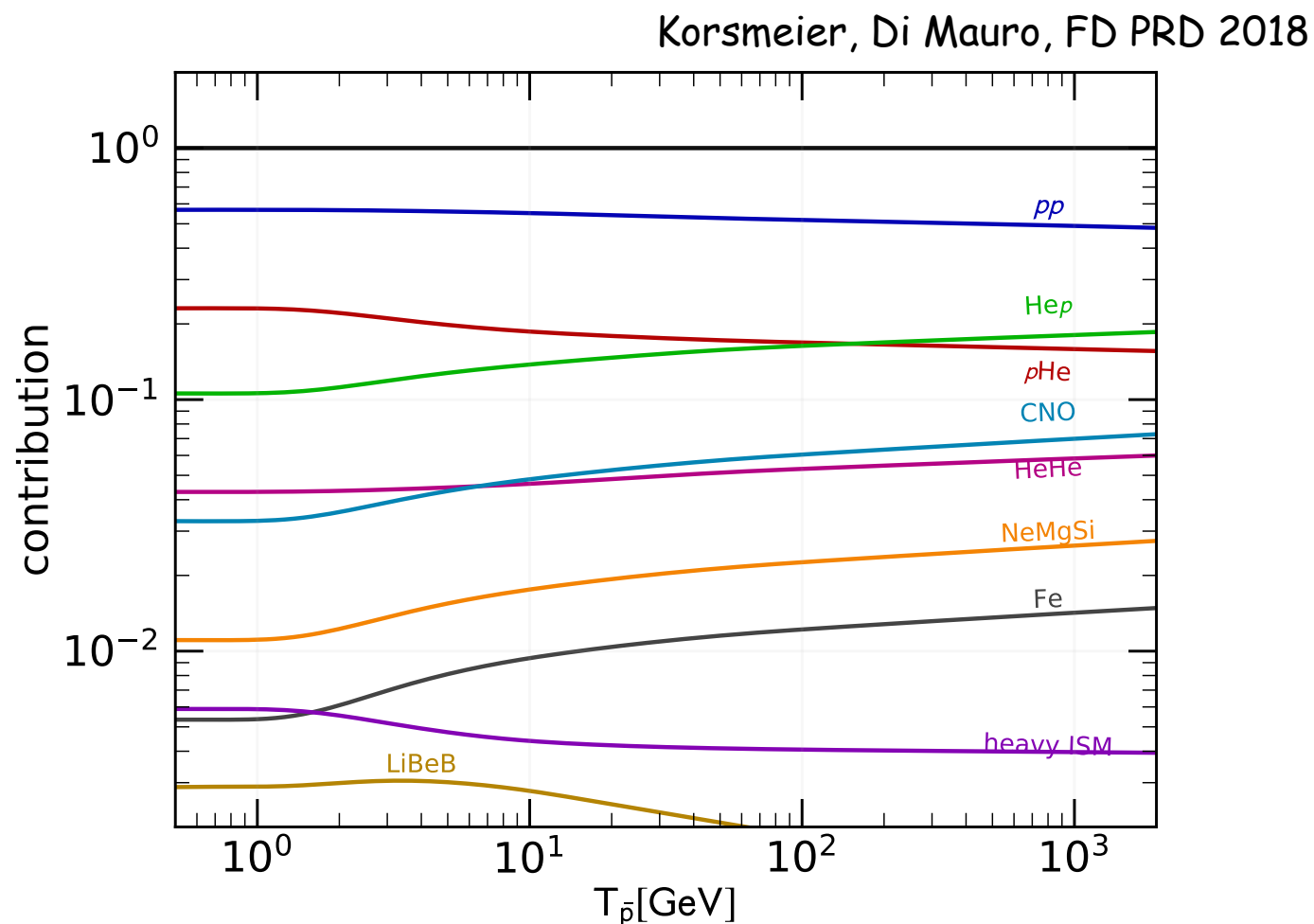
Channel	min	mean	max
$^{12}\text{C} \rightarrow ^{11}\text{B}$	30.8	32.7	35.3
$^{16}\text{O} \rightarrow ^{11}\text{B}$	16.2	17.7	18.8
$^{12}\text{C} \rightarrow ^{10}\text{B}$	9.04	9.95	10.9
$^{16}\text{O} \rightarrow ^{10}\text{B}$	7.64	8.17	8.68
$^{12}\text{C} \rightarrow ^{11}\text{B} \rightarrow ^{10}\text{B}$	2.07	2.16	2.26
$^{16}\text{O} \rightarrow ^{12}\text{C} \rightarrow ^{11}\text{B}$	1.60	1.96	2.34
$^{16}\text{O} \rightarrow ^{15}\text{N} \rightarrow ^{11}\text{B}$	1.29	1.69	2.04
$^{24}\text{Mg} \rightarrow ^{11}\text{B}$	1.51	1.59	1.69
$^{20}\text{Ne} \rightarrow ^{11}\text{B}$	1.26	1.32	1.39
$^{14}\text{N} \rightarrow ^{11}\text{B}$	1.00	1.32	1.66
$^{28}\text{Si} \rightarrow ^{11}\text{B}$	0.85	1.29	1.66
$^{16}\text{O} \rightarrow ^{11}\text{B} \rightarrow ^{10}\text{B}$	1.03	1.17	1.26
$^{16}\text{O} \rightarrow ^{13}\text{C} \rightarrow ^{11}\text{B}$	0.54	1.15	1.62
$^{16}\text{O} \rightarrow ^{14}\text{N} \rightarrow ^{11}\text{B}$	0.68	0.83	0.92
$^{24}\text{Mg} \rightarrow ^{10}\text{B}$	0.66	0.75	0.84
$^{16}\text{O} \rightarrow ^{12}\text{C} \rightarrow ^{10}\text{B}$	0.51	0.59	0.69
$^{16}\text{O} \rightarrow ^{15}\text{N} \rightarrow ^{10}\text{B}$	0.50	0.59	0.68
$^{20}\text{Ne} \rightarrow ^{10}\text{B}$	0.47	0.54	0.63
$^{28}\text{Si} \rightarrow ^{10}\text{B}$	0.32	0.53	0.67
$^{14}\text{N} \rightarrow ^{10}\text{B}$	0.39	0.50	0.65
$^{56}\text{Fe} \rightarrow ^{11}\text{B}$	0.11	0.49	1.10
$^{16}\text{O} \rightarrow ^{13}\text{C} \rightarrow ^{10}\text{B}$	0.12		

A silhouette of a person in a dark jacket and hat is shown from the side, looking through a large telescope mounted on a tripod. The background is a clear night sky filled with stars and the Milky Way galaxy, which appears as a bright, hazy band of light stretching across the sky. The text "The case for antimatter" is overlaid in a bright yellow, sans-serif font.

The case for
antimatter

Nuclei contributions to antiprotons

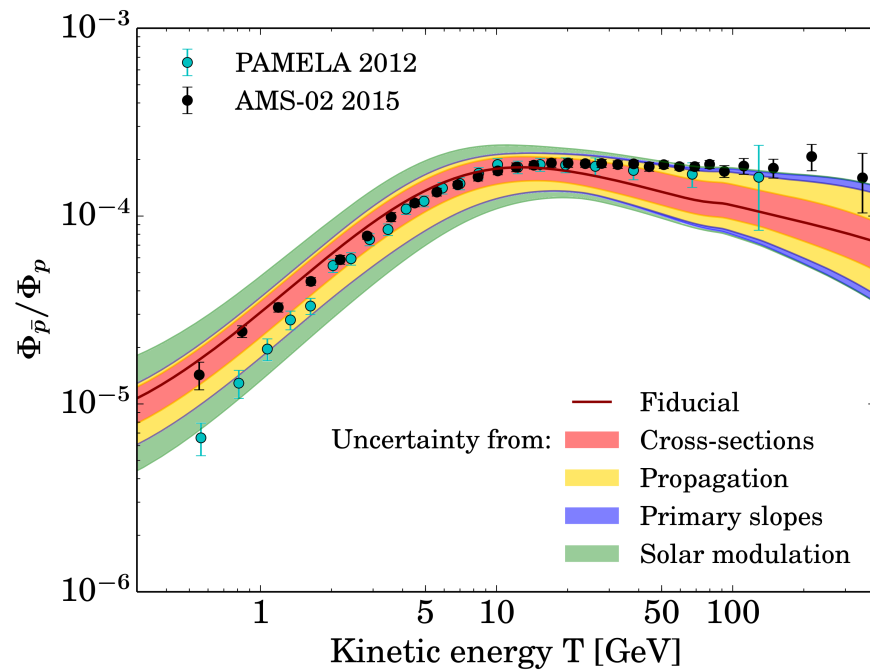
Relevant contribution of the different channels to the total production of antiprotons in the Galaxy (CR-ISM)



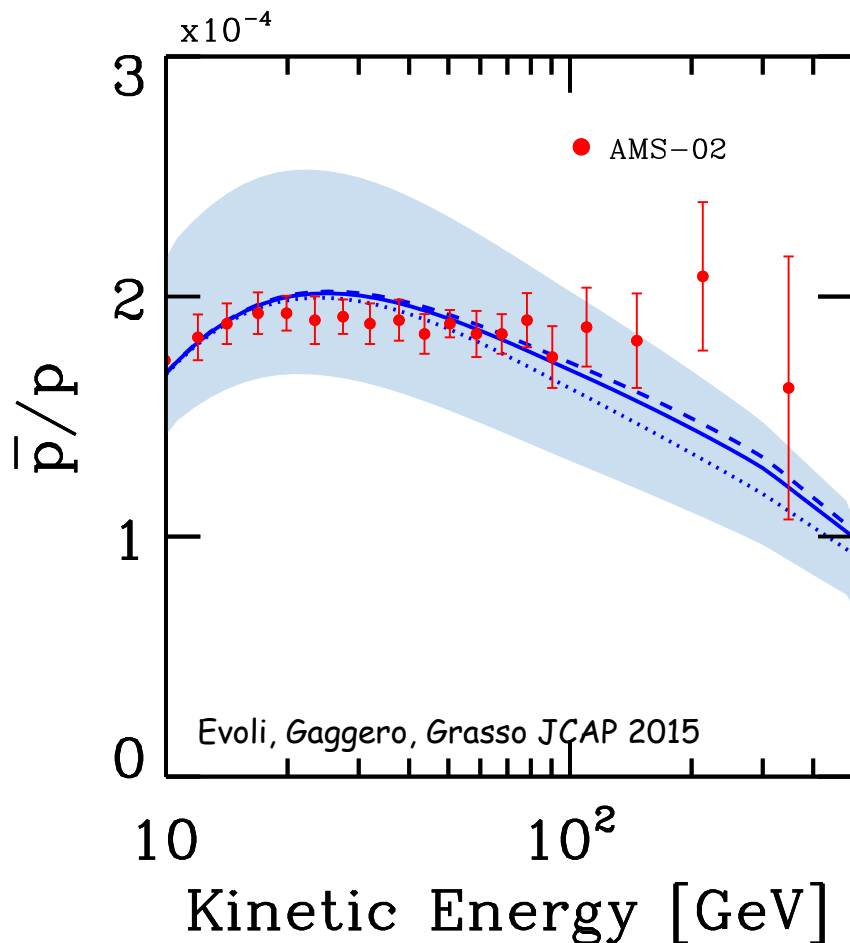
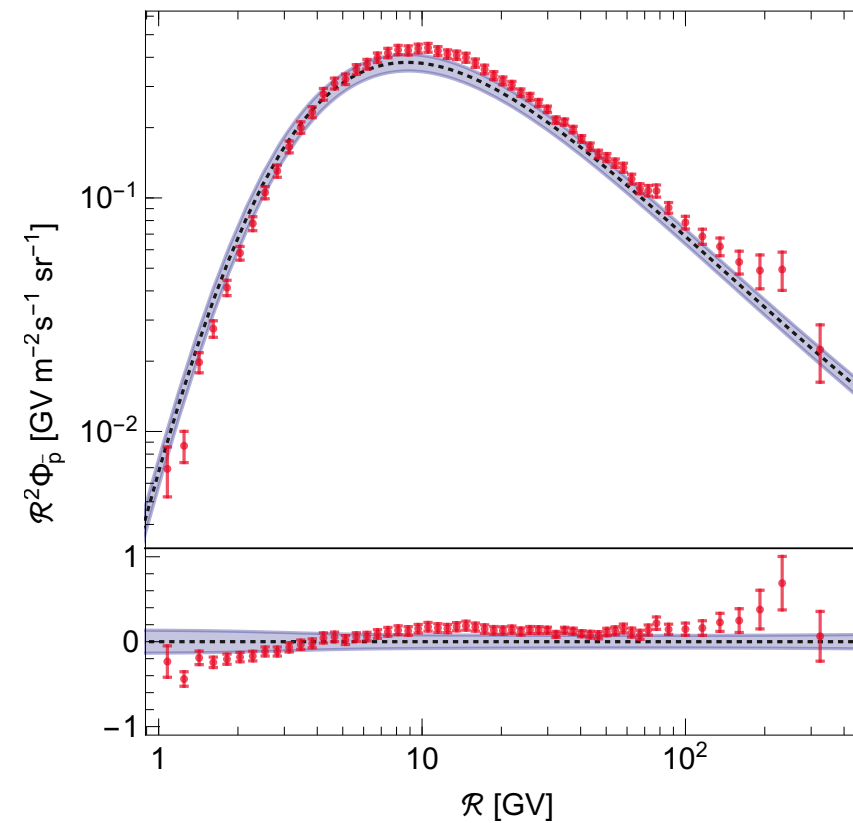
The channels involving He - both CR and ISM target - contribute 30-40% to the antiproton source in the Galaxy

Interpretation of antiproton data

Giesen + JCAP 2015



Reinert & Winkler JCAP 2018



Propagation models fitted on AMS-02 B/C data. Greatest uncertainty set by nuclear cross sections.

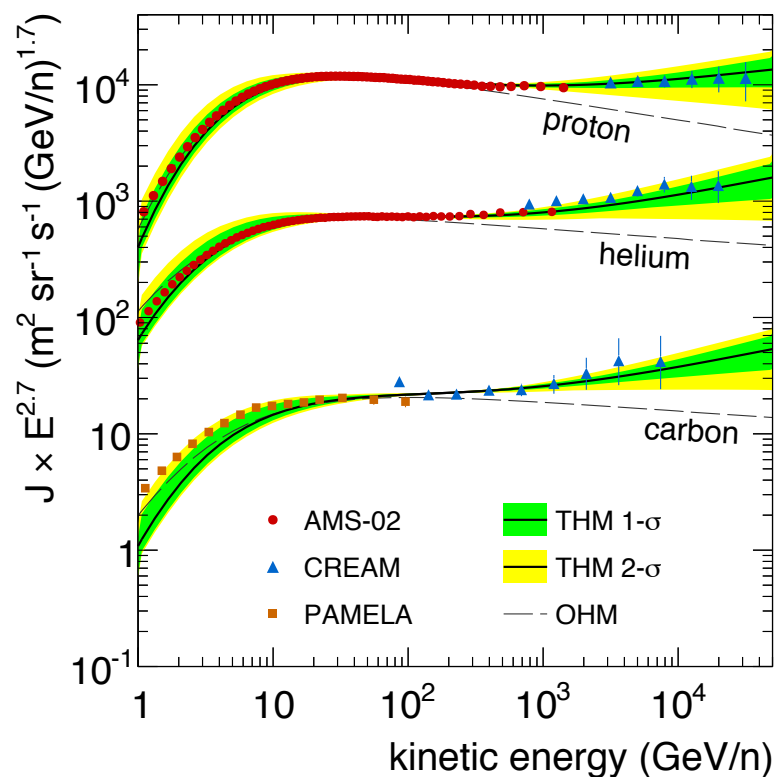
Background antiproton can explain data naturally, mainly because of the small diffusion coefficient slope indicated by B/C.

Two halo transport model

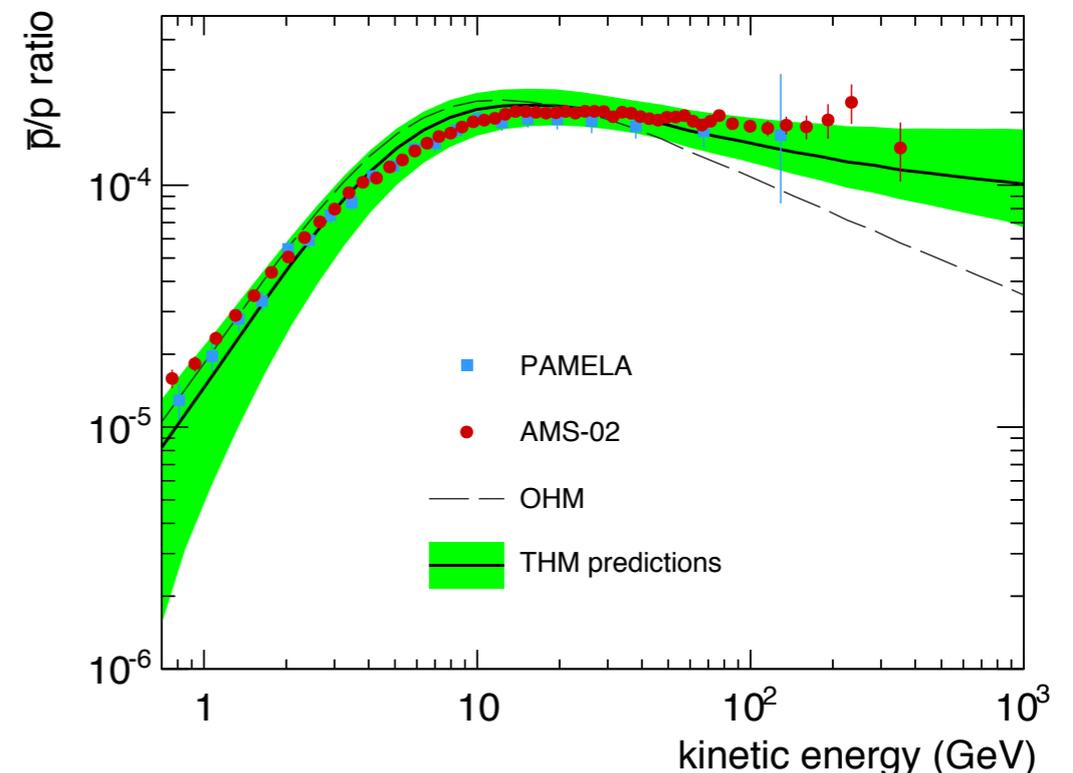
Tomassetti ApJ 2012, PRD 2015

Cosmic rays are allowed to experience a different type of diffusion when they propagate closer to the Galactic plane

$$D(\mathcal{R}, z) = \begin{cases} D_0 \beta^\eta \left(\frac{\mathcal{R}}{\mathcal{R}_0} \right)^\delta & (|z| < \xi L) \\ \chi D_0 \beta^\eta \left(\frac{\mathcal{R}}{\mathcal{R}_0} \right)^{\delta+\Delta} & (|z| > \xi L) \end{cases}$$



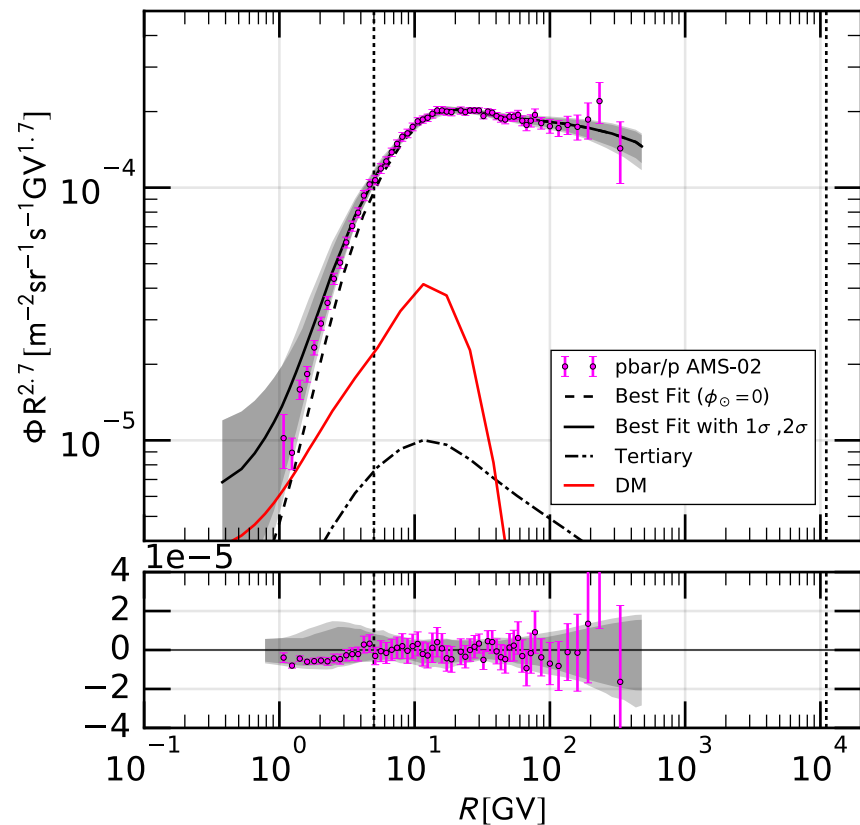
Feng, Tomassetti, Oliva PRD2016



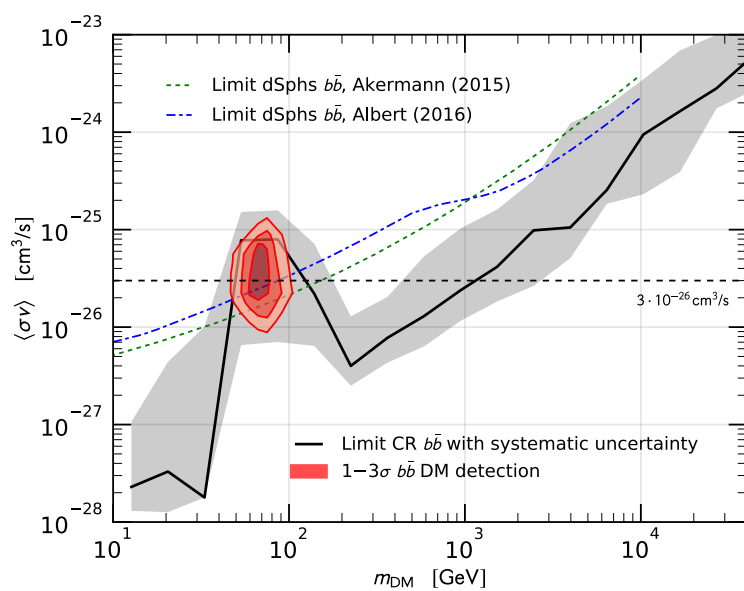
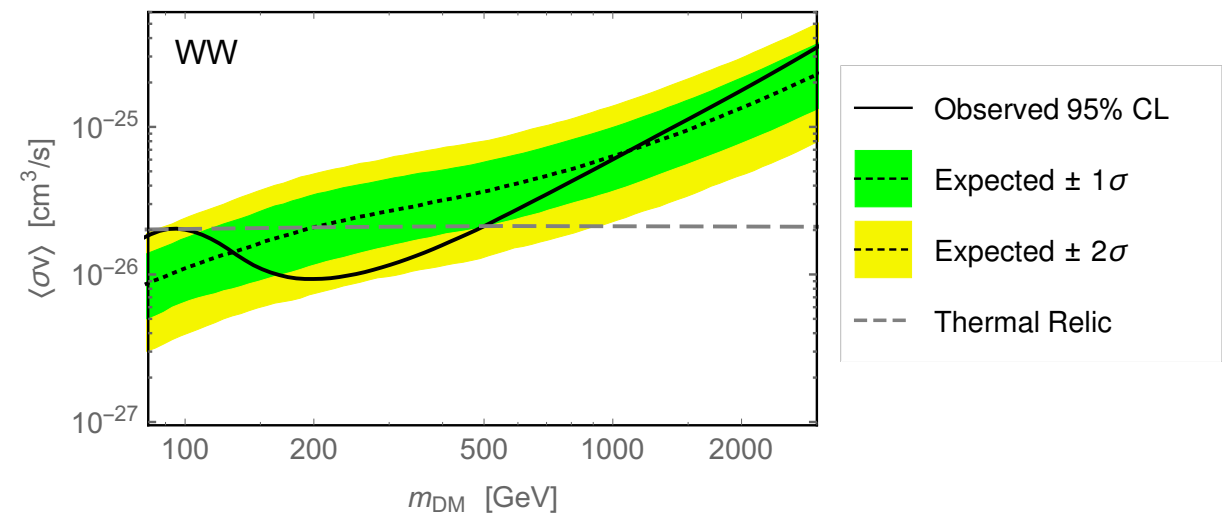
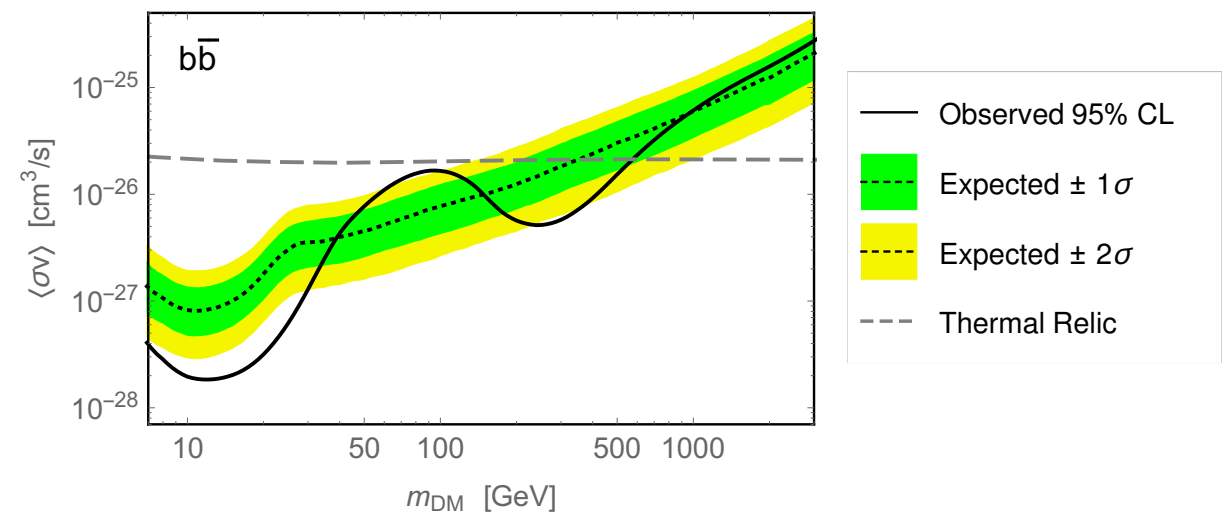
Antiprotons and other species are consistent with the 2 halo model

Possible contribution from dark matter

Cuoco, Korsmeier, Kraemer PRL 2017



Reinert & Winkler JCAP2018



Antiproton data are so precise that permit to set strong upper bounds on the dark matter annihilation cross section, or to improve the fit w.r.t. to the secondaries alone adding a fine DM contribution

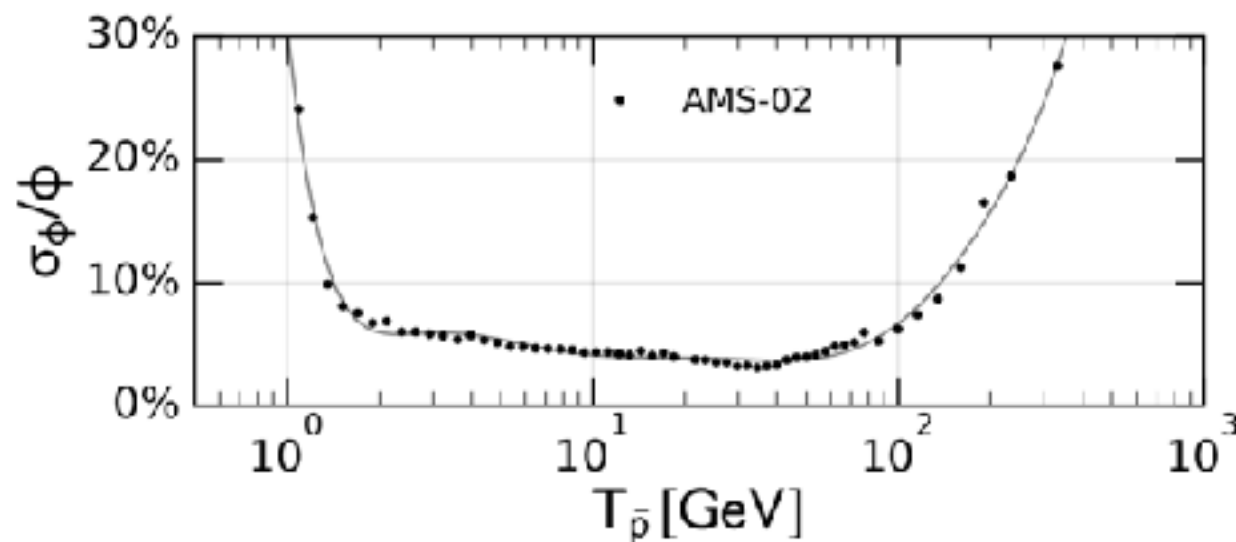
Antiproton production cross sections

FD, Korsmeier, Di Mauro PRD 2017

$$q_{ij}(T_{\bar{p}}) = \int_{T_{\text{th}}}^{\infty} dT_i 4\pi n_{\text{ISM},j} \phi_i(T_i) \frac{d\sigma_{ij}}{dT_{\bar{p}}}(T_i, T_{\bar{p}})$$

Source term

$i, j = \text{proton, helium}$
(both in the CRs and in the ISM)



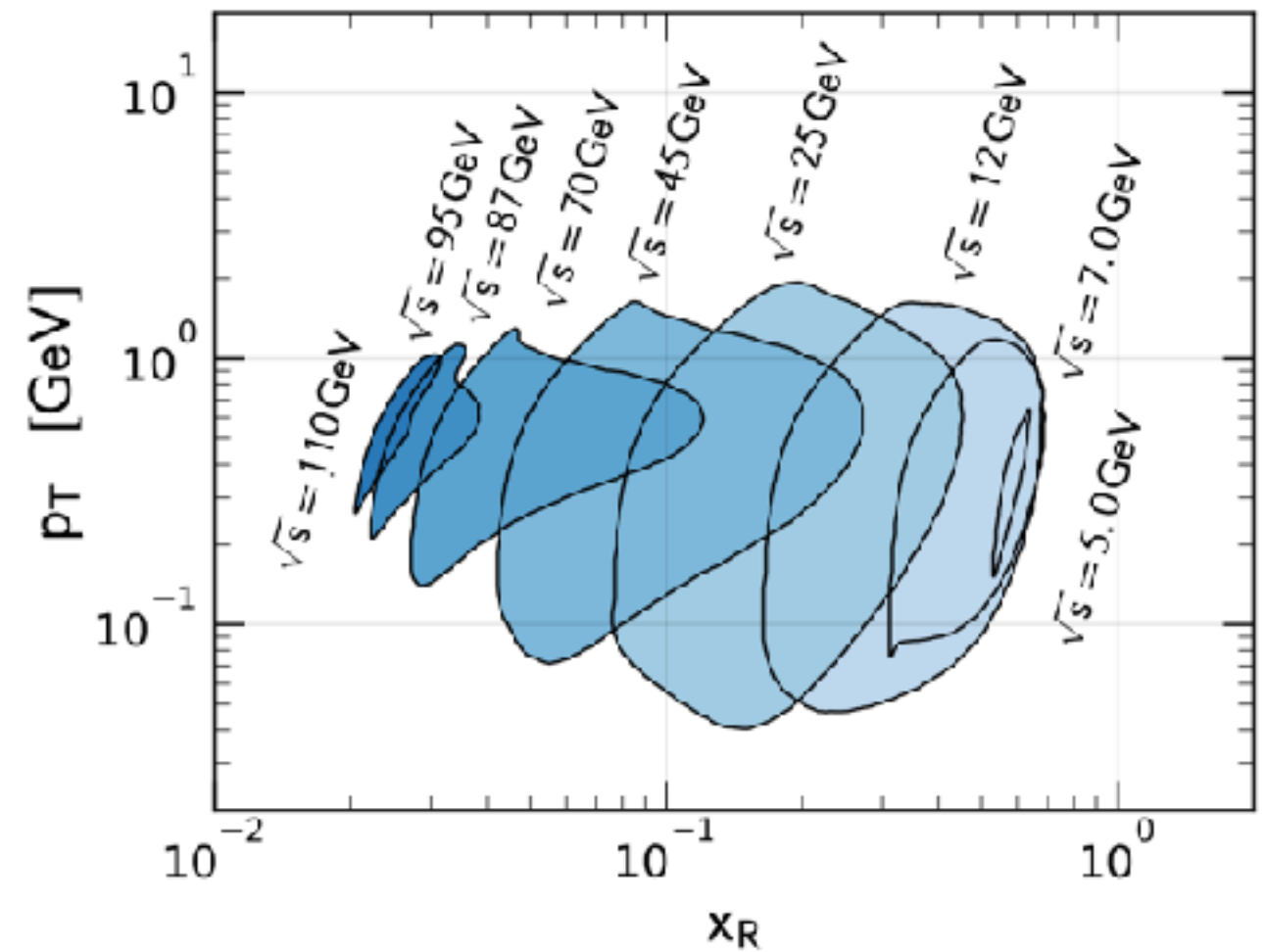
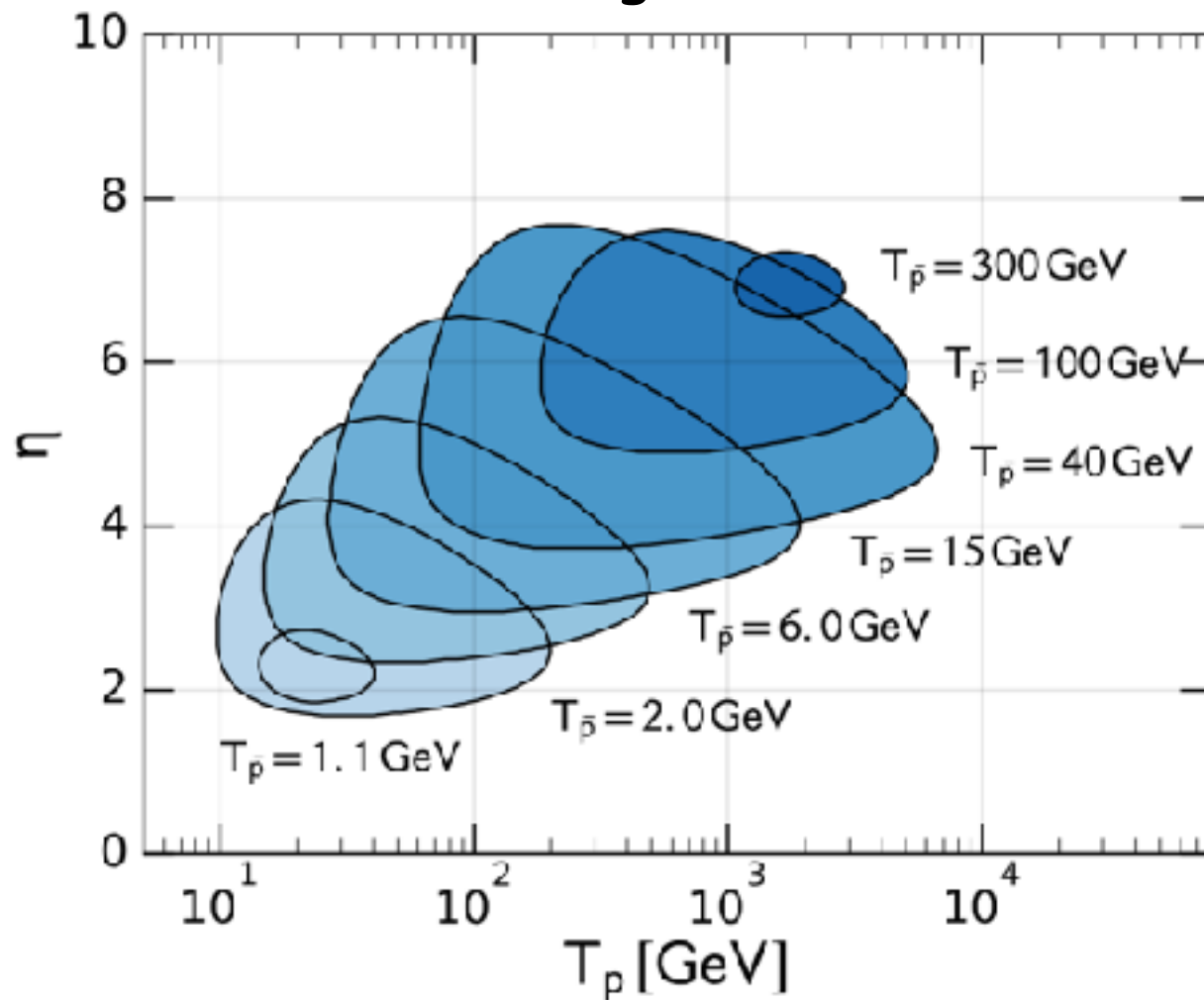
**Cosmic antiproton data are very precise:
production cross sections should be known with high accuracy
in order not to introduce high theoretical uncertainties**

Parameter space to be covered by future high energy experiments

FD, Korsmeier, Di Mauro PRD 2017

Lab frame

Fixed target



AMS02 accuracy is reached if $pp \rightarrow p\bar{p}$ cross section is measured with 3% accuracy inside the regions, 30% outside.

New fixed-target data for the antiproton XS

Korsmeier, FD, Di Mauro, PRD 2018

$pp \rightarrow p\bar{p} + X$

NA61 (Aduszkiewicz Eur. Phys. J. C77 (2017))

$\sqrt{s} = 7.7, 8.8, 12.3$ and 17.3 GeV

$T_p = 31, 40, 80, 158$ GeV

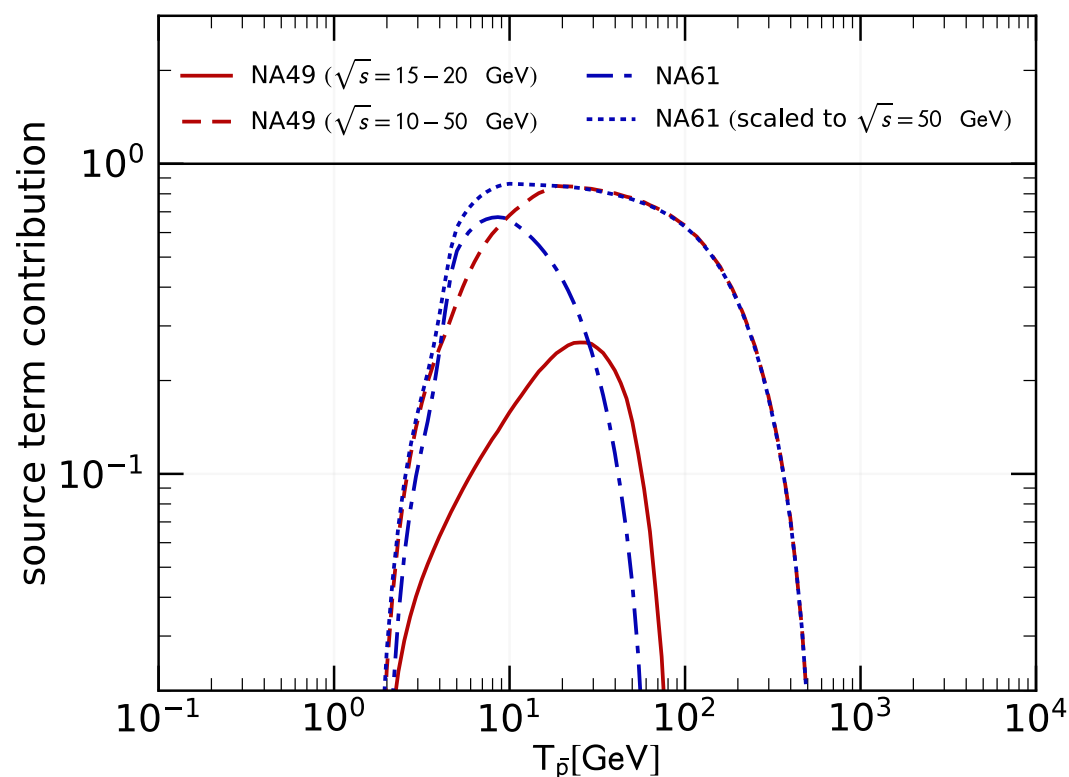
$p\text{He} \rightarrow p\bar{p} + X$

LHCb (Graziani et al. Moriond 2017)

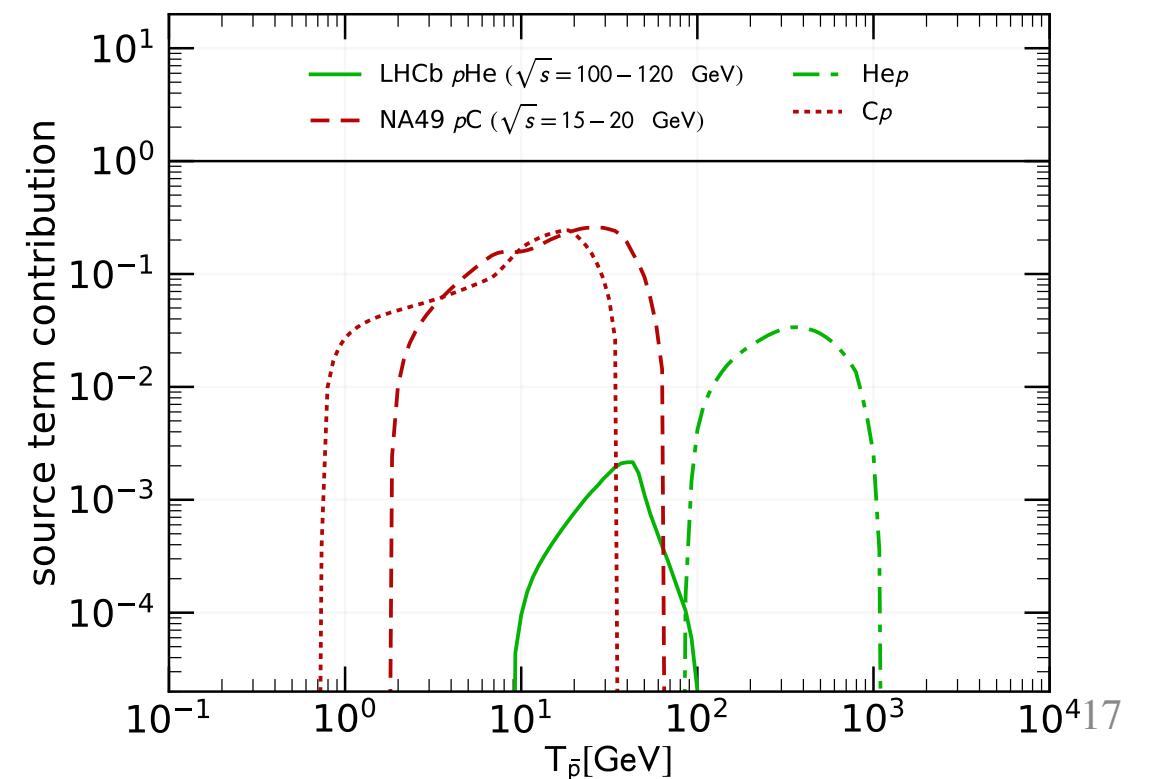
$\sqrt{s} = 110$ GeV

$T_p = 6.5$ TeV

Fraction of the pp source term covered by the kinematical parameters space



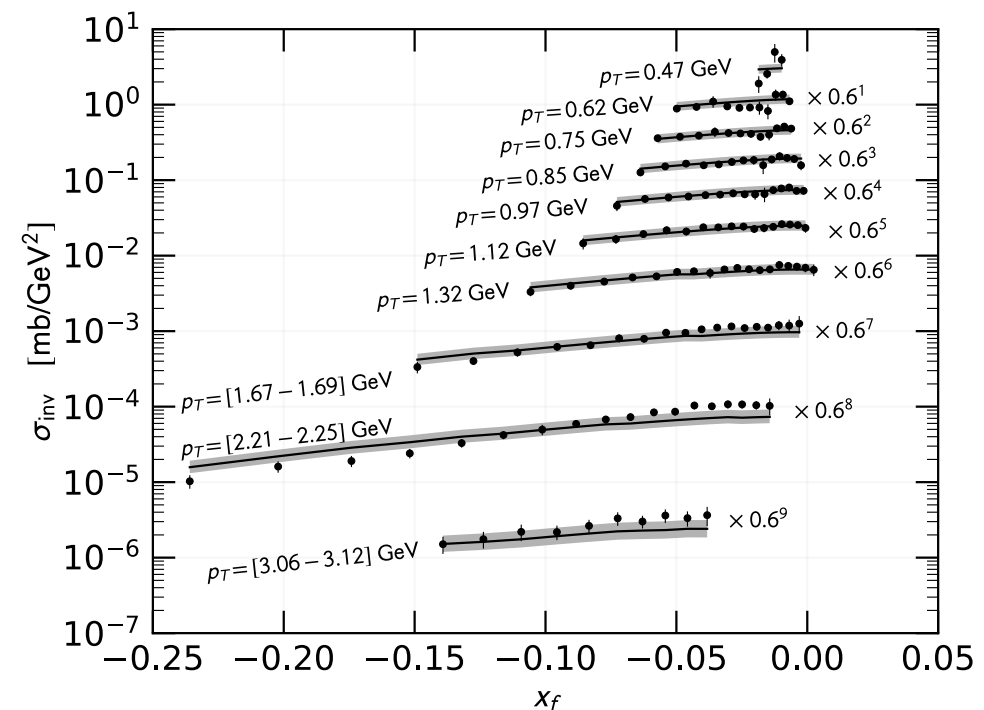
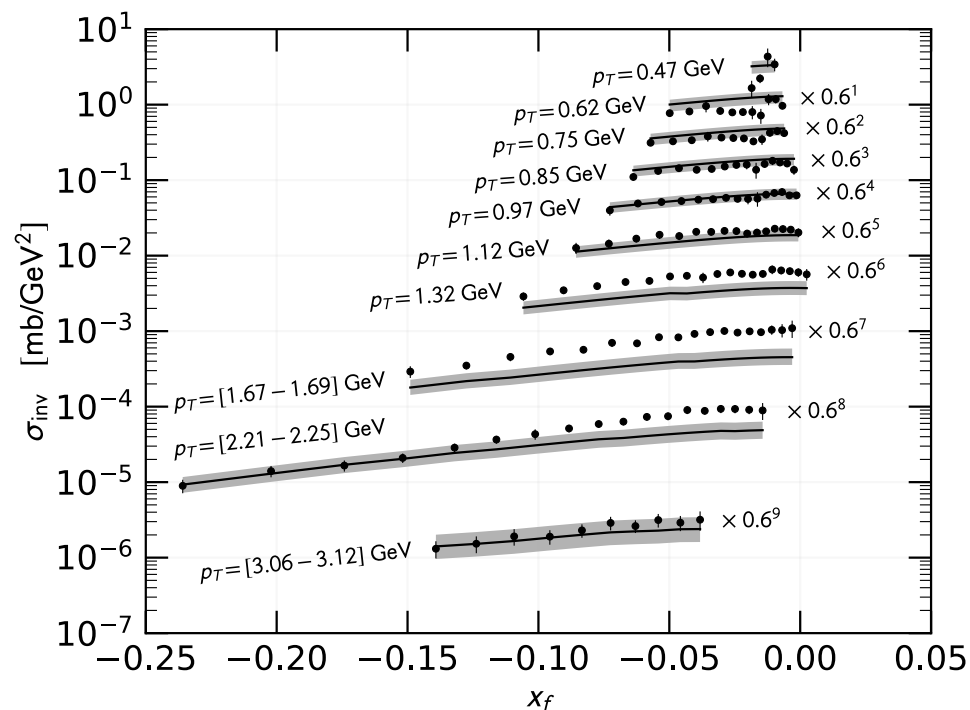
Fraction of the p-nucleus source term covered by the kinematical parameters space



New high energy data analysis

Korsmeier, FD, Di Mauro, PRD 2018

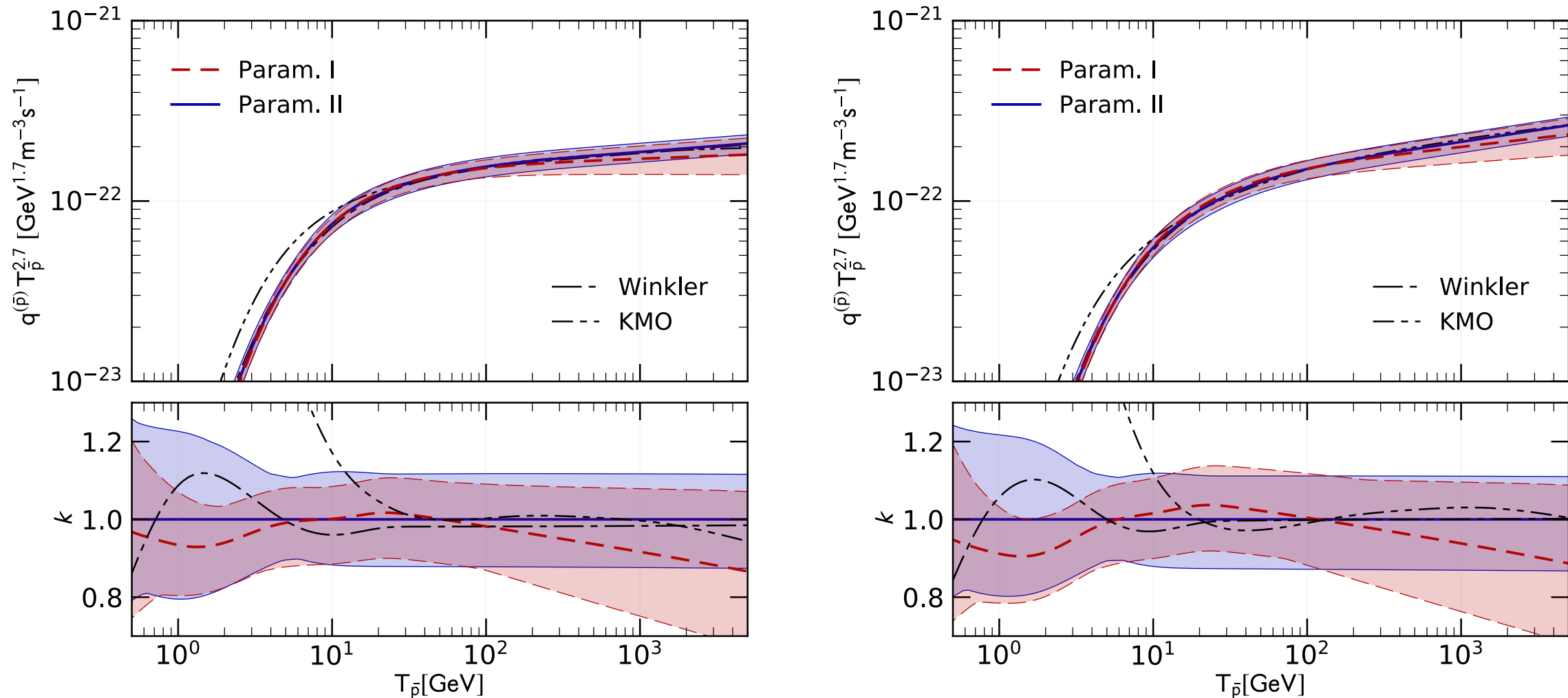
1. Fit to NA61 pp \rightarrow pbar + X data
2. Calibration of pA XS on NA49 pC \rightarrow pbar + X data
3. Inclusion of LHC pHe \rightarrow pbar + X data



LHCb data agree better with one of the two pp parameterizations. They select the high energy behavior of the Lorentz invariant cross section

The antiproton source spectrum

Korsmeier, FD, Di Mauro PRD 2018



Param II is preferred by the fits.

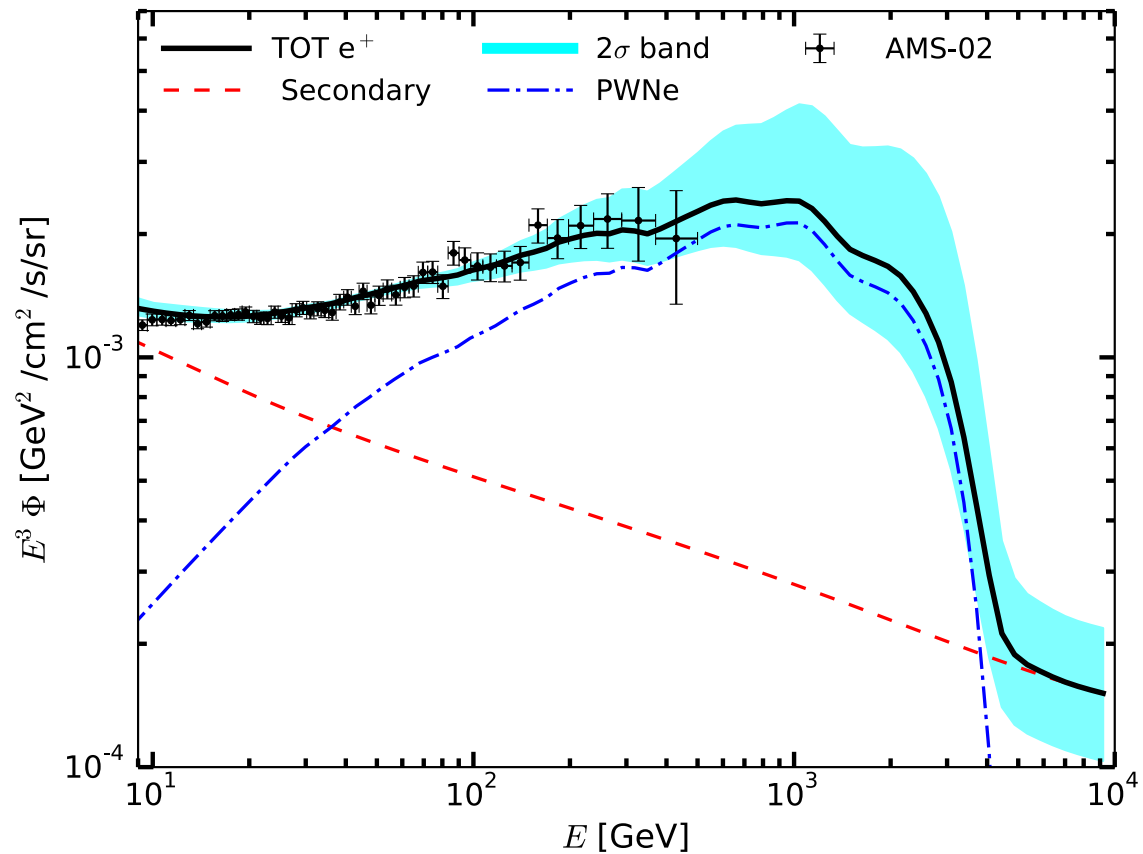
The effect of LHCb data is to select a h.e. trend of the pbar source term.

A harder trend is preferred.

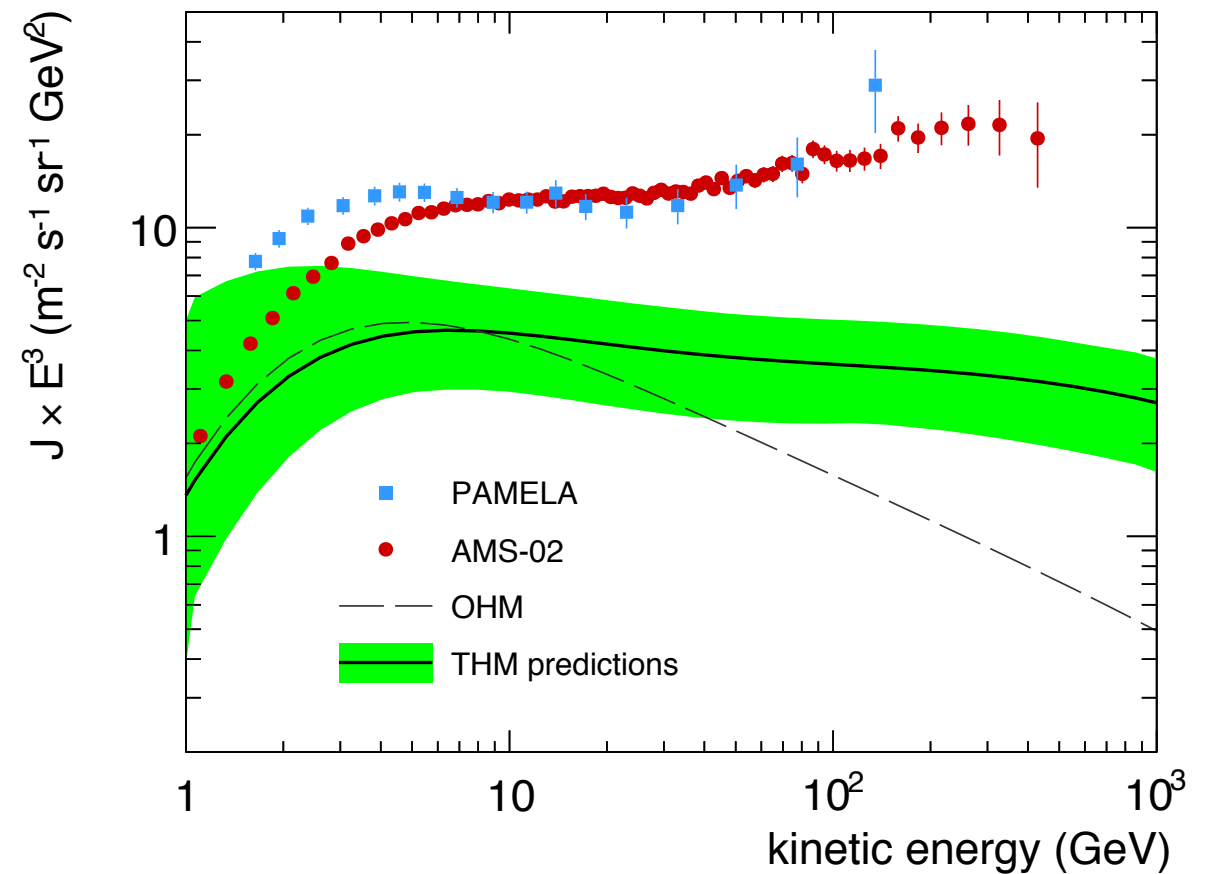
Uncertainties still range about 20%, and increase at low energies.

The cosmic positrons

Manconi, FD, Di Mauro JCAP 2017



Feng, Tomassetti, Oliva PRD 2017



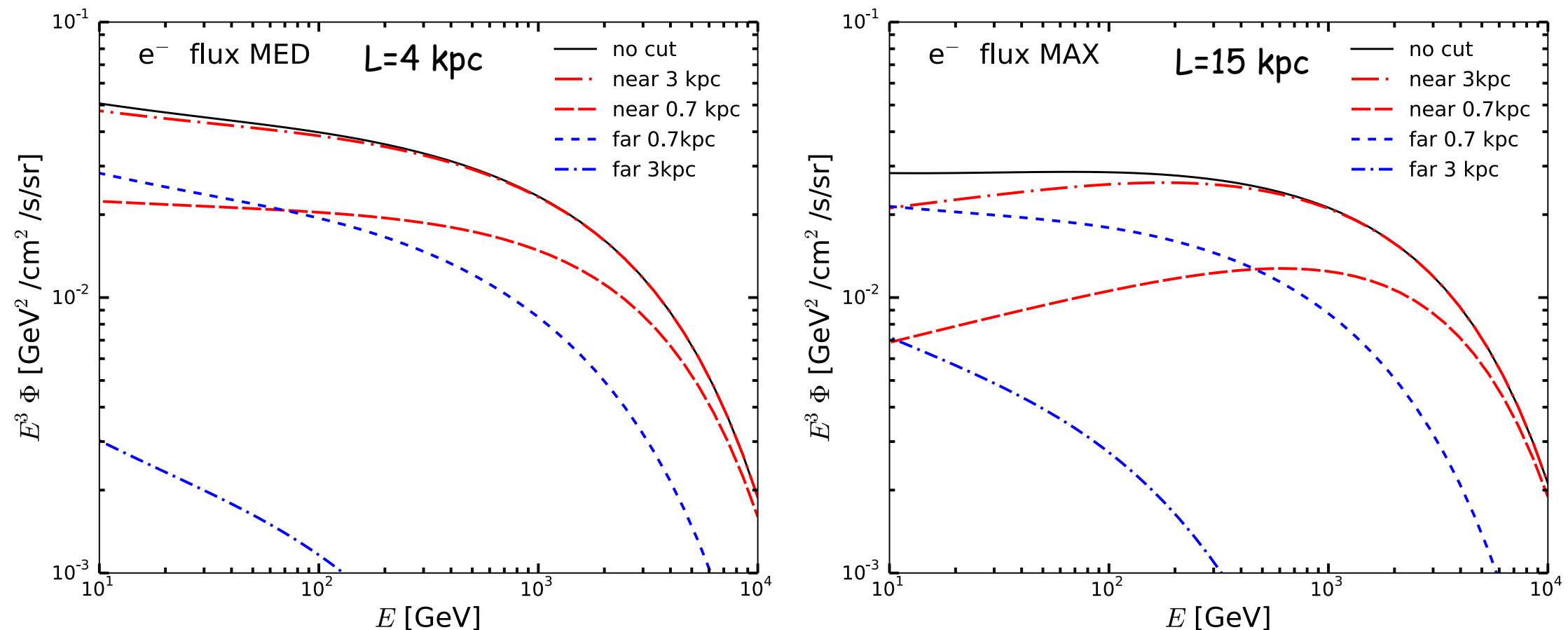
Secondary positrons predicted in realistic transport models cannot explain alone the positron flux.

One or more components are needed, typically in nearby sources given the strong radiative cooling experienced by e^+e^- .

Far and near sources: contributions

Manconi, Di Mauro, FD JCAP 2017

Electrons (positrons) at the Earth



Most of the electrons from a (Green 2015) **smooth SNR** distribution come from very few kpc from the Earth. Less than 10% of e⁻ come from $R > 3$ kpc, even considering a large size L for the diffusive halo.

We can consider separately a smooth SNR distribution out of a R_{cut} , and single (catalog) **SNR** and **PWN** inside that circle.

A multi-wavelength, multi-messenger analysis

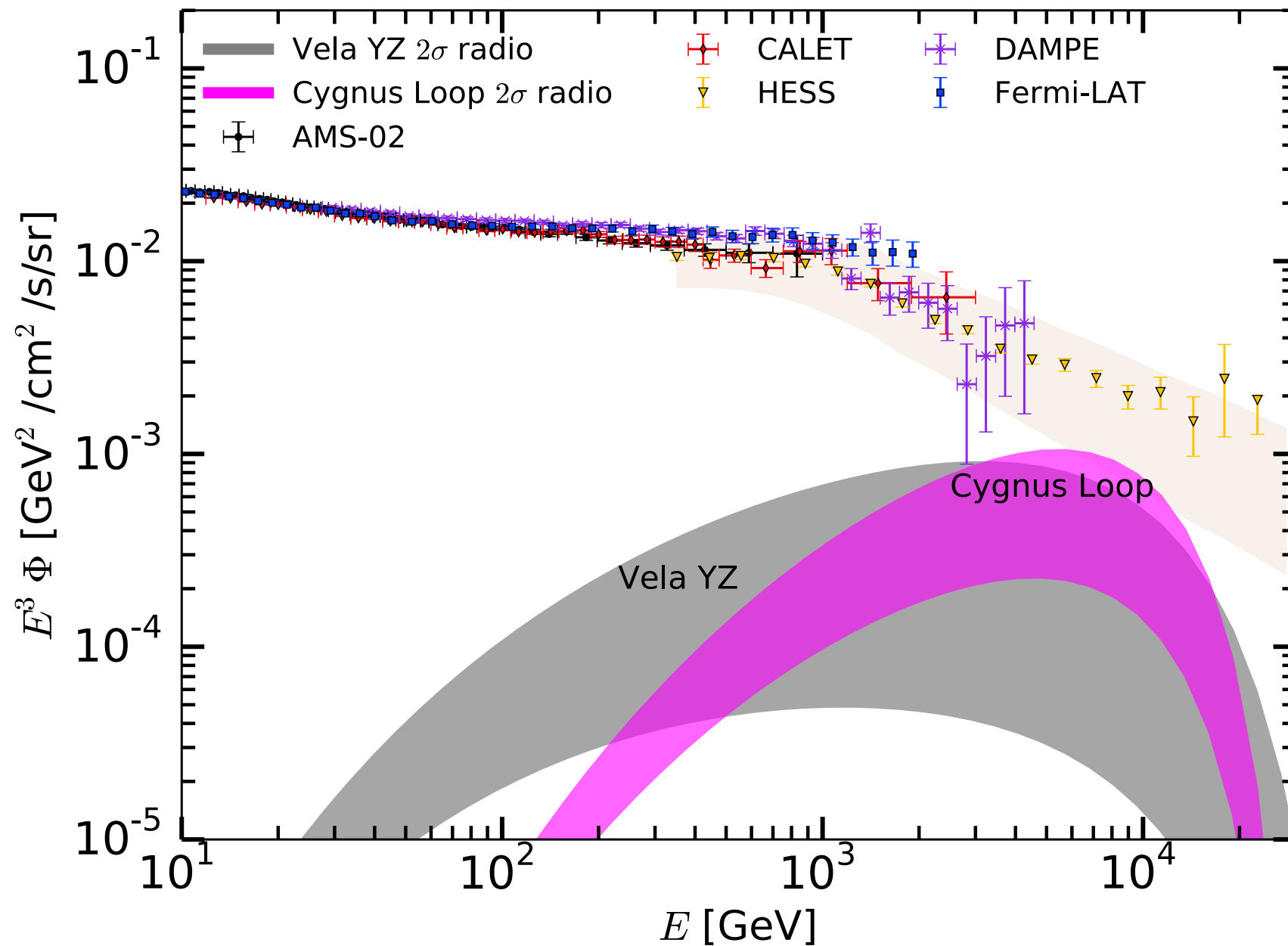
S. Manconi, M. Di Mauro, FD 1803:01009 PRD subm.

We build a model for the production and propagation of e^- and e^+ in the Galaxy and test it against 3 observables:

1. **Radio brightness data** from Vela YZ and Cygnus Loop at all frequencies.
The radio emission is all synchrotron from e^- accelerated by the source
2. **e^+e^- flux** from 5 experiments, **e^+ flux** from AMS
Far and near SNRs, near SNRs and PWNe, secondaries for e^+e^- .
The e^+ flux constrains the PWN emission.
 e^+e^- data taken with their uncertainty on the energy scale.
3. **e^+e^- dipole anisotropy** upper bounds from Fermi-LAT
Test on the power of this observable on the closest SNRs.

Vela YZ and Cygnus Loop contribution to e^+e^-

S. Manconi, M. Di Mauro, FD 1803:01009

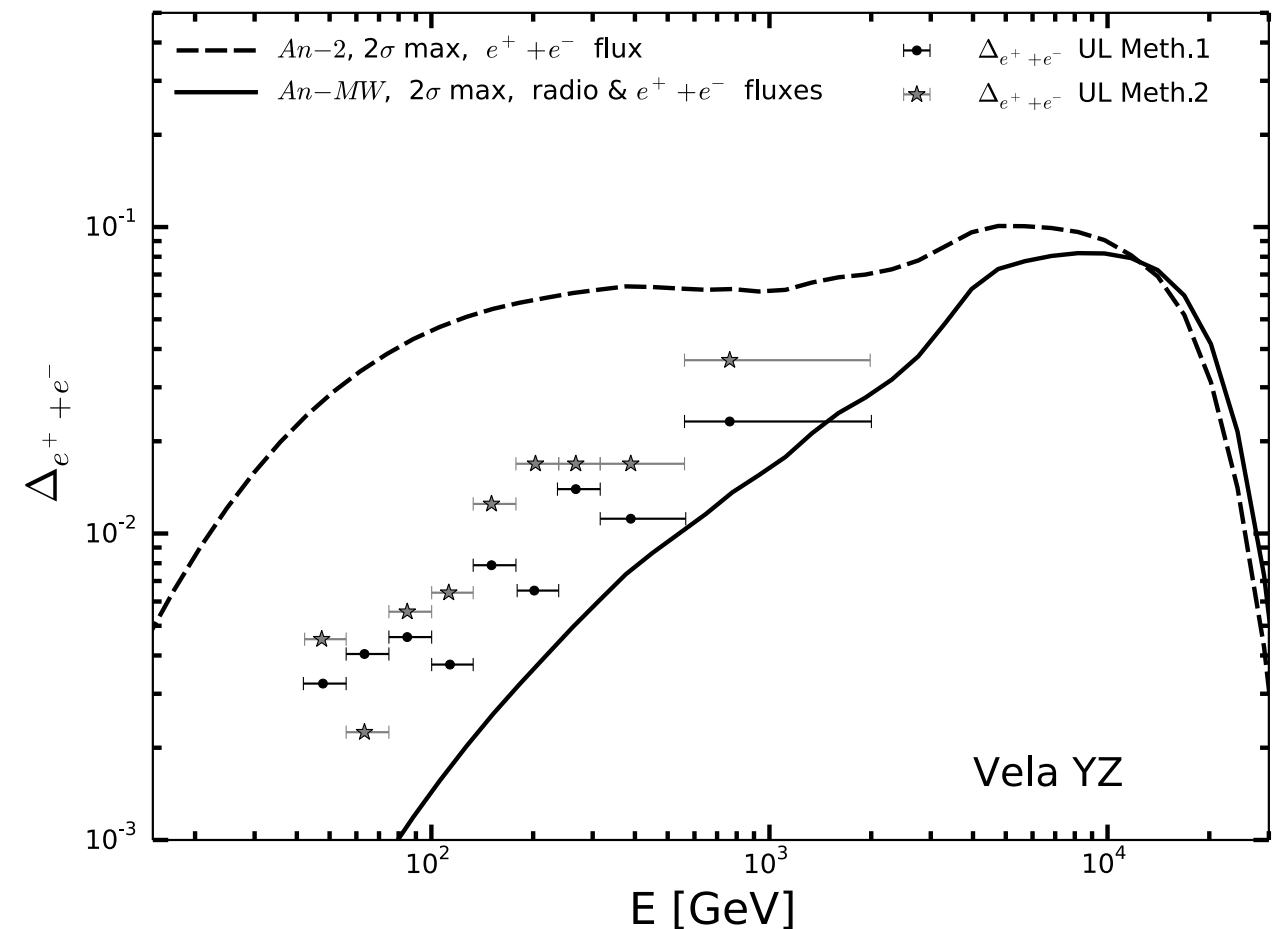
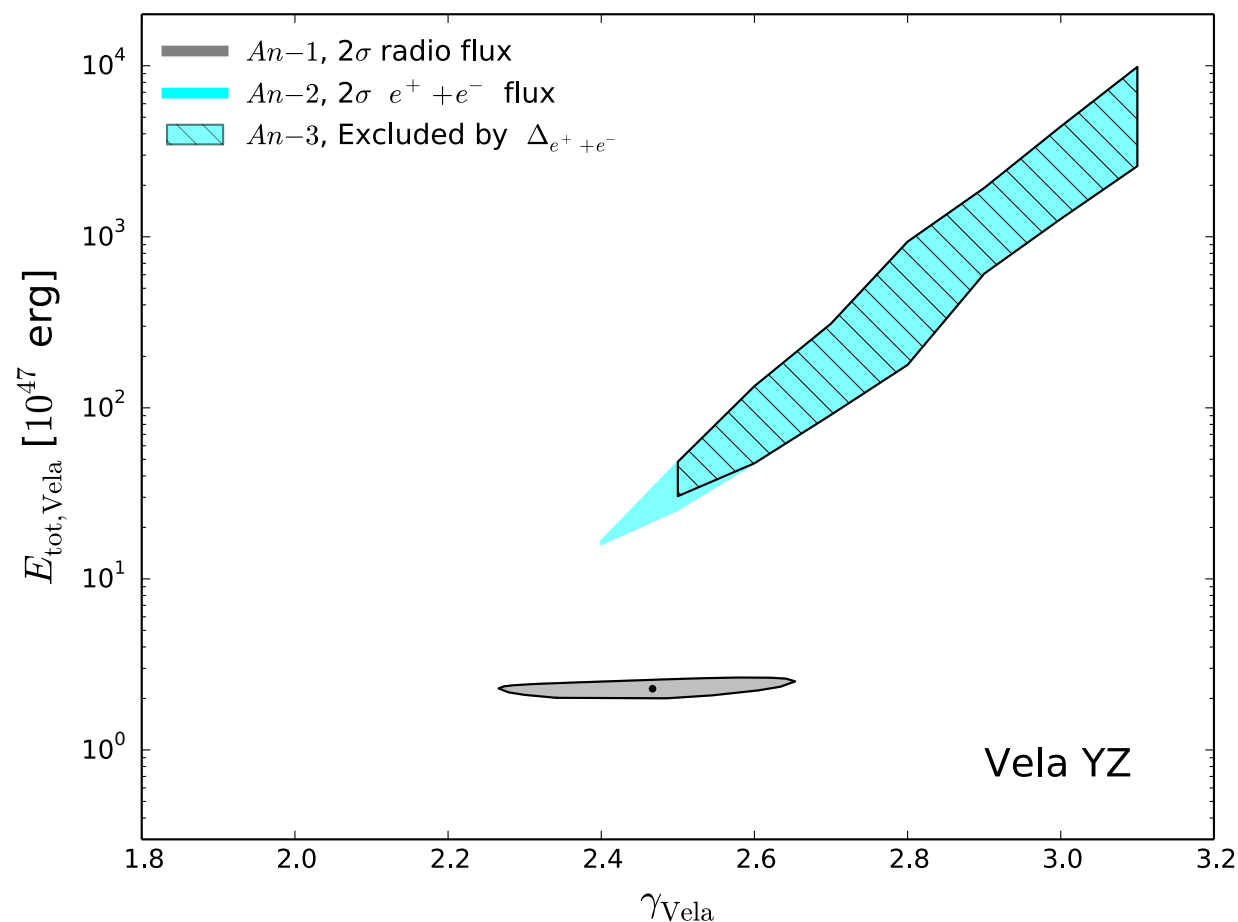


Radio data from the SNRs, at all available frequencies, constrain Vela and Cygnus e^- emission to be below the present data

Vela YZ SNR properties and anisotropies

S. Manconi, M. Di Mauro, FD 1803:01009

$$Q(E) = Q_0 \left(\frac{E}{E_0} \right)^{-\gamma} \exp \left(-\frac{E}{E_c} \right) \quad E_{\text{tot}} = \int_{E_1}^{\infty} dE E Q(E)$$

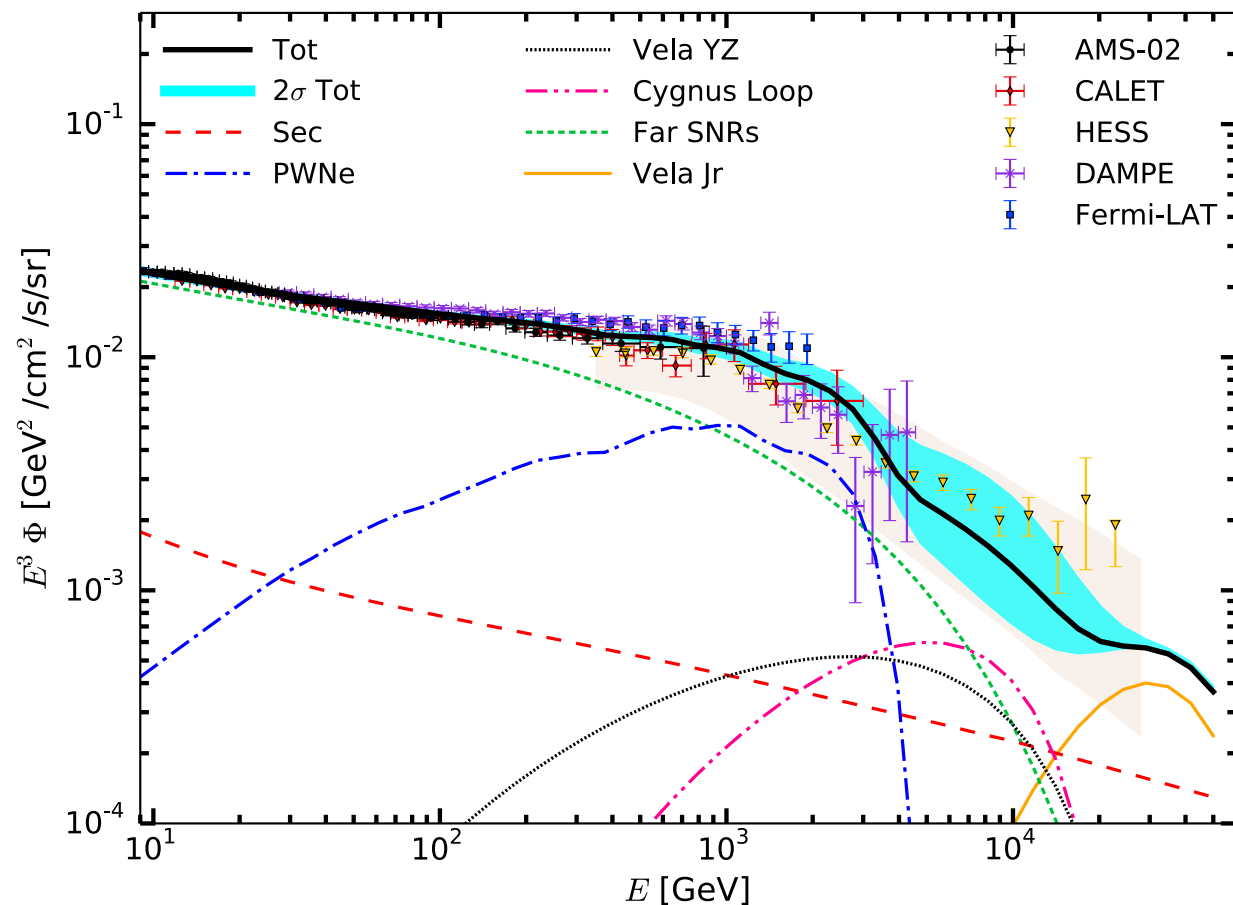


1. Radio data are very selective
2. e^+e^- and e^+ fluxes well fitted
3. Dipole anisotropy excludes configs

- The constraints from e^+e^- fit give an exceeding dipole anisotropy.
- Radio data AND e^+e^- flux are compatible with anisotropy

The recent $e^+ e^-$ data and a unique model

S. Manconi, M. Di Mauro, FD 1803:01009



Recent data from 5 experiments

Fit with:

1. Smooth far (>0.7 kpc) SNR (e^-)
2. Near Vela YZ and Cygnus SNR (e^-)
3. Near PWNe ($e^+ e^-$)
4. Secondaries on the ISM ($e^+ e^-$)

We can fit the whole data (9 free parameters + sol. mod.) with a consistent model provided that the proper systematic errors on the **energy scale** of each experiment are included

Different physical contributions shape non trivial slope changes

Conclusions

- The secondary nuclei brings unique information on the transport properties in the Galaxy and the production in local sites.
- Very precise antimatter data are now tested against very refined models, including possible contribution from dark matter
- The lepton fluxes can be understood in a composite framework of smooth and single sources
- A new challenge is astronomy with charged particles